DOC

EPA

United States
Department of
Commerce

National Oceanic and Atmospheric Administration
Environmental Research Laboratories
Seattle WA 98115

United States
Environmental Protection
Agency

Office of Energy, Minerals, and
Industry
Washington DC 20460

EPA-600/7-79-165
July 1979

Research and Development

A Study of the Dispersal of Suspended Sediment from the Fraser and Skagit Rivers into Northern Puget Sound Using LANDSAT Imagery

Interagency Energy/Environment R&D Program Report

RESEARCH REPORTING SERIES

Research reports of the Office of Research and Development, U.S. Environmental Protection Agency, have been grouped into nine series. These nine broad categories were established to facilitate further development and application of environmental technology. Elimination of traditional grouping was consciously planned to foster technology transfer and a maximum interface in related fields. The nine series are:

1. Environmental Health Effects Research
2. Environmental Protection Technology
3. Ecological Research
4. Environmental Monitoring
5. Socioeconomic Environmental Studies
6. Scientific and Technical Assessment Reports (STAR)
7. Interagency Energy-Environment Research and Development
8. "Special" Reports
9. Miscellaneous Reports

This report has been assigned to the INTERAGENCY ENERGY-ENVIRONMENT RESEARCH AND DEVELOPMENT series. Reports in this series result from the effort funded under the 17-agency Federal Energy/Environment Research and Development Program. These studies relate to EPA's mission to protect the public health and welfare from adverse effects of pollutants associated with energy systems. The goal of the Program is to assure the rapid development of domestic energy supplies in an environmentally-compatible manner by providing the necessary environmental data and control technology. Investigations include analyses of the transport of energy-related pollutants and their health and ecological effects; assessments of, and development of, control technologies for energy systems; and integrated assessments of a wide range of energy-related environmental issues.

This document is available to the public through the National Technical Information Service, Springfield, Virginia 22161.

A STUDY OF THE DISPERSAL OF SUSPENDED SEDIMENT FROM THE FRASER AND SKAGIT RIVER INTO NORTHERN PUGET SOUND USING LANDSAT IMAGERY

by

Richard A. Feely and Marilyn F. Lamb

Pacific Marine Environmental Laboratory
Environmental Research Laboratories
National Oceanic and Atmospheric Administration
7600 Sand Point Way N.E.
Seattle, Washington 98115

Prepared for the MESA (Marine Ecosystems Analysis) Puget Sound Project, Seattle, Washington in partial fulfillment of

EPA Interagency Agreement No. D6-E693-EN
Program Element No. EHE625-A

This study was conducted
as part of the Federal
Interagency Energy/Environment
Research and Development Program

Prepared for

OFFICE OF ENERGY, MINERALS, AND INDUSTRY
OFFICE OF RESEARCH AND DEVELOPMENT
U.S. ENVIRONMENTAL PROTECTION AGENCY
WASHINGTON, D.C. 20460

February 1979

Completion Report Submitted to
PUGET SOUND ENERGY-RELATED RESEARCH PROJECT
MARINE ECOSYSTEMS ANALYSIS PROGRAM
ENVIRONMENTAL RESEARCH LABORATORIES

by

Pacific Marine Environmental Laboratory
Environmental Research Laboratories
National Oceanic and Atmospheric Administration
7600 Sand Point Way N.E.
Seattle, Washington 98115

This work is the result of research sponsored by the Environmental Protection Agency and administered by the Environmental Research Laboratories of the National Oceanic and Atmospheric Administration.

The Environmental Research Laboratories do not approve, recommend, or endorse any proprietary product or proprietary material mentioned in this publication. No reference shall be made to the Environmental Research Laboratories or to this publication furnished by the Environmental Research Laboratories in any advertising or sales promotion which would indicate or imply that the Environmental Research Laboratories approve, recommend, or endorse any proprietary product or proprietary material mentioned herein, or which has as its purpose an intent to cause directly or indirectly the advertised product to be used or purchased because of this Environmental Research Laboratories publication.

CONTENTS

Figures iv
Tables vi

1. Introduction 1

1.1 General Statement 1
1.2 Program Rationale and Objectives 2

2. Geography, Physical Oceanography, and Hydrology 3

2.1 Physiographic Setting 3
2.2 Circulation Patterns and Hydrography 3
2.3 River Runoff and Sediment Discharge 5

3. Conclusions 11

3.1 LANDSAT Imagery 11
3.2 Quantitative Sediment Mapping 11

4. Recommendations 12

5. Methodology 13

5.1 General Statement 13
5.2 LANDSAT Imagery and Hydrographic Data 13
5.3 Sea-Truth Measurements 16
5.4 MSS Computer Compatible Tapes 16

6. Results and Discussion 17

6.1 Seasonal Variations of Sediment Dispersal 17
6.2 Tidal Variations of Sediment Dispersal 28
6.3 Density Fronts 30
6.4 Quantitative Sediment Mapping 33

7. Summary and Conclusions 41

Acknowledgments 43
Bibliography 44

FIGURES

Number		Page
2.1	Physical setting of the study region	4
2.2	Monthly range, mean, and standard deviation of: a. water discharge; and b. suspended sediment discharge for the Fraser River at Hope, B.C. for the period from 1967 through 1977	8
2.3	Monthly mean discharge of water and suspended sediments of the Skagit River at Mt. Vernon during 1975	10
5.1	Locations of sampling stations for sea truth measurements	15
6.1	MSS Band 5 of LANDSAT image 1169-18373 on Jan. 8, 1973 between slack water and minor ebb current	18
6.2	MSS Band 5 of LANDSAT image 1187-18374 on Jan. 26, 1973	19
6.3	MSS Band 4 of LANDSAT image 2417-18220 on Mar. 14, 1976	20
6.4	MSS Band 5 of LANDSAT image 2111-18254 showing a southeasterly dispersal of suspended sediments from the Fraser River into the Strait of Georgia on May 13, 1975	21
6.5	MSS Band 5 of LANDSAT image 2129-18254 showing a southwesterly dispersal of suspended sediments from the Fraser River into the Strait of Georgia on May 31, 1975	22
6.6	MSS Band 5 of LANDSAT image 1727-18290 showing a southeasterly dispersal of suspended sediments from the Fraser River into the Strait of Georgia on July 20, 1974	23

Number		Page
6.7	MSS Band 5 of LANDSAT image 5465-17484 showing a southeasterly dispersal of suspended sediments from the Fraser River into the Strait of Georgia on July 27, 1976	24
6.8	MSS Band 4 of LANDSAT image 2921-18025 showing southeasterly dispersal of suspended sediments from the Fraser River into the Strait of Georgia on July 31, 1977	25
6.9	MSS Band 5 of LANDSAT image 2957-18004 showing a southwesterly dispersal of suspended sediments from the Fraser River into the Strait of Georgia on Sept. 5, 1977	26
6.10	MSS Band 5 of LANDSAT image 21227-18025 showing a southeasterly dispersal from the Fraser River into the Strait of Georgia on June 2, 1978	27
6.11	Schematic diagram of a vertical section normal to a density front	30
6.12	Low altitude aerial photograph showing sharp color boundary of a density front	31
6.13a	Composite sketch of fronts seen in 24 LANDSAT images during ebb tides	32
6.13b	Composite sketch of fronts seen in 9 LANDSAT images during flood tides	32
6.14	Scatter plots of the relationships among Band 5 image radiance from the LANDSAT multispectral scanner	37
6.15	Upwelled radiance for Calvert clay and Ball clay	39
6.16	Total suspended matter contour maps as determined from computer analysis of LANDSAT images	40

TABLES

Number		Page
2.1	Average annual runoff from the major rivers discharging into the study region	6
2.2	Comparison of mean water and sediment discharge for the Fraser and Skagit Rivers during period of record (1967-1977)	7
5.1	Principal characteristics of the LANDSAT satellite and multispectral scanner	14
6.1	Results of sea truth measurements and remotely sensed radiances for selected locations near the mouths of the Fraser and Skagit Rivers	34
6.2	Correlation coefficient matrix and linear regression equation for total suspended matter (TSM) in northern Puget Sound	35
6.3	Results of the stepwise regression analysis of the radiance data from the MSS computer compatible tapes with the sea-truth measurements of total suspended matter	35
6.4	Correlation coefficient matrix and linear regression equation for inorganic suspended matter (ISM) in northern Puget Sound	36
6.5	Results of the stepwise regression analysis of the radiance data from the MSS computer compatible tapes with the sea-truth measurements of inorganic suspended matter	36

1. INTRODUCTION

1.1 GENERAL STATEMENT

With the recent development of petroleum reserves at Prudhoe Bay and the projected development of petroleum and natural gas reserves on the OCS of Alaska, northern Puget Sound and the Strait of Juan de Fuca-Strait of Georgia system are slated to become a major transportation route through which Alaskan crude oils are delivered to Washington State refineries. Refining of petroleum is presently carried out at Cherry Point, Ferndale, and Anacortes refineries. Associated with increased production of the refineries will be the exportation of refined products to markets outside the State of Washington. A portion of the products undoubtedly will be transported by water, thus creating an increased potential for hydrocarbon loading of the local marine waters through minor spillage or a major tanker accident.

With few notable exceptions, the region has not been plagued with massive oil spills, although the effects of chronic, low-level inputs of petroleum and refined products have not been adequately assessed. In the past, tanker and barge traffic in the region has been minimal because much of the imported crude oil arrived by pipeline from Canada. However, plans announced by the National Energy Board of Canada will systematically reduce and finally terminate all exports of crude oil by 1982 (EPA, 1977). This action will result in a significant increase in tanker traffic to meet local domestic needs. While the various options for allocation and transportation of Alaskan crude oil to West Coast ports are presently being discussed, it remains clear that ever increasing amounts of petroleum will be moved through the Strait of Juan de Fuca and San Juan Passages via tankers to meet local demands.

Once crude oil and petroleum products are introduced into the marine environment, a combination of physical, chemical, and biological processes become operative in the breakdown and removal of the oil. These processes include spreading, dispersion, atmospheric injection, evaporation, chemical and biological emulsification, and sorption onto particles (NAS, 1975). The last process is one of particular interest because it represents a means by which oil can be carried down into the water column and become available for interaction with marine organisms.

Since crude oil is sparingly soluble in seawater, it tends to form emulsions when introduced into seawater, especially under intense wave action. The emulsions have a high affinity for particles and tend to be adsorbed rapidly. Recent studies of oil spills in coastal waters containing high suspended loads have indicated rapid removal of oil by sorption onto particles along frontal zones (Forrester, 1971 and Klemas and Polis, 1977). These zones are regions where turbid brackish water contacts seawater. At the interface downwelling occurs in most cases, causing the inorganic material from the rivers and any associated contaminants to be carried down into the water column. Similarly, laboratory studies involving the interaction between crude oils and river-derived inorganic suspended matter have indicated

that significant amounts of oil may be accommodated by suspended material, and that the quantity of oil retained on the particles is dependent upon the isolectric point of oil and sediment particles, particle size, temperature, and the concentration of the oil relative to that of the suspended material (Baker et al., 1978; Feely et al., 1978). Since these processes play a major role in the disposal and deposition of petroleum hydrocarbons, this study addresses the temporal and spatial distributions of suspended matter emanating from the Fraser and Skagit Rivers by means of careful analysis of LANDSAT imagery.

1.2 PROGRAM RATIONALE AND OBJECTIVES

Several recent advances in remote sensing techniques have provided scientists with the ability to collect synoptic information about water circulation and sediment dispersal patterns which heretofore have been unobtainable. The multispectral scanner images from the LANDSAT-1 and LANDSAT-2 satellites have been especially useful for the study of suspended matter transport processes in coastal and estuarine water (Kritkos et al., 1974; Klemas et al., 1974; Gatto, 1976; Johnson et al., 1977).

A number of investigators have attempted to produce suspended matter distribution maps based on density-sliced photographic images and sea-truth determinations (Sharma et al., 1974; Carlson et al., 1975). These investigations demonstrated the difficult problems of obtaining reproducible information from photographic images. However, recent investigations of the relationships between suspended matter concentrations in the upper 1 m of the water column and image radiance using computer compatible tapes have proved to be successful if the ambient suspended matter concentrations were sufficiently high, such as the waste water disposal area in the New York Bight Apex (Johnson et al., 1977). These results suggest that computer compatible tapes of LANDSAT imagery can be combined with sea-truth data to obtain algorithms for mapping suspended matter concentrations.

The primary objectives of this study are to: (1) describe the dispersal patterns of suspended matter emanating from the Fraser and Skagit Rivers by means of careful analysis of LANDSAT imagery; and (2) to develop and evaluate computer algorithms for mapping concentrations of total and inorganic suspended matter from the Fraser and Skagit Rivers.

2. GEOGRAPHY, PHYSICAL OCEANOGRAPHY, AND HYDROLOGY

2.1 PHYSIOGRAPHIC SETTING

Figure 2.1 shows the physical setting of the study region. The area is an inland sea with access to the open Pacific Ocean through two major waterways, the Strait of Georgia and the Strait of Juan de Fuca. The Strait of Georgia, to the north, is one of the largest inland waterways on the west coast of North America. It is partially enclosed with Vancouver Island forming the western boundary and the mainland of British Columbia and northwestern Washington forming the eastern boundary. The Strait of Georgia is about 220 km long, 33 km wide, and has an average depth of about 150 m. The San Juan Archipelago and the Canadian Gulf Islands separate the Strait of Georgia from the Strait of Juan de Fuca. Passage between these major waterways is primarily accomplished through Haro Strait to the west and Rosario Strait to the east.

The Strait of Juan de Fuca, to the south, is a submarine valley extending from the Pacific Ocean to Whidbey Island and Rosario Strait, about 145 km long. The width varies between 20 and 24 km from the entrance to the Port Angeles area, where it narrows to 16 km near Victoria, B.C., before widening to about 40 km. The Strait contains two basins which are separated by a cross-channel ridge or sill. The ridge extends southward from Victoria, at an approximate depth of 60 m. The western basin or Outer Strait slopes gradually in a seaward direction. The eastern basin or Inner Strait contains several channels which lead into Haro Strait, Rosario Strait, and Admiralty Inlet.

2.2 CIRCULATION PATTERNS AND HYDROGRAPHY

Circulation patterns and hydrography for the study region have been studied and reviewed by several authors (Tully, 1942; Waldichuk, 1957; Herlinveaux and Tully, 1961; Chang et al., 1976; Parker, 1977; Schumacher et al., 1978), and only a brief summary is deemed necessary for the purpose of this report.

The primary factors that control circulation and the distribution of properties in the study region include tides, fresh water runoff, winds and atmospheric pressure variations, with secondary influences due to coriolis force, centrifugal force, and topography. The Strait of Georgia is characterized by a strong vertical stratification which results from fresh water input from numerous mainland rivers, the Fraser River being the major contributor. Driven by estuarine flow, the brackish water moves progressively seaward, primarily through the San Juan passages into the Strait of Juan de Fuca, where mixing occurs as a result of turbulent tidal energy. As the brackish water mixes with the saline Pacific Ocean water, part of it is returned to the deeper waters of the Strait of Georgia. However, the major portion escapes to the Pacific Ocean in the upper layer. Salt balance is maintained by the intrusion of colder, more saline water from the Pacific at mid-depths in the Strait of Juan de Fuca during the summer months (Waldichuk, 1957). This water

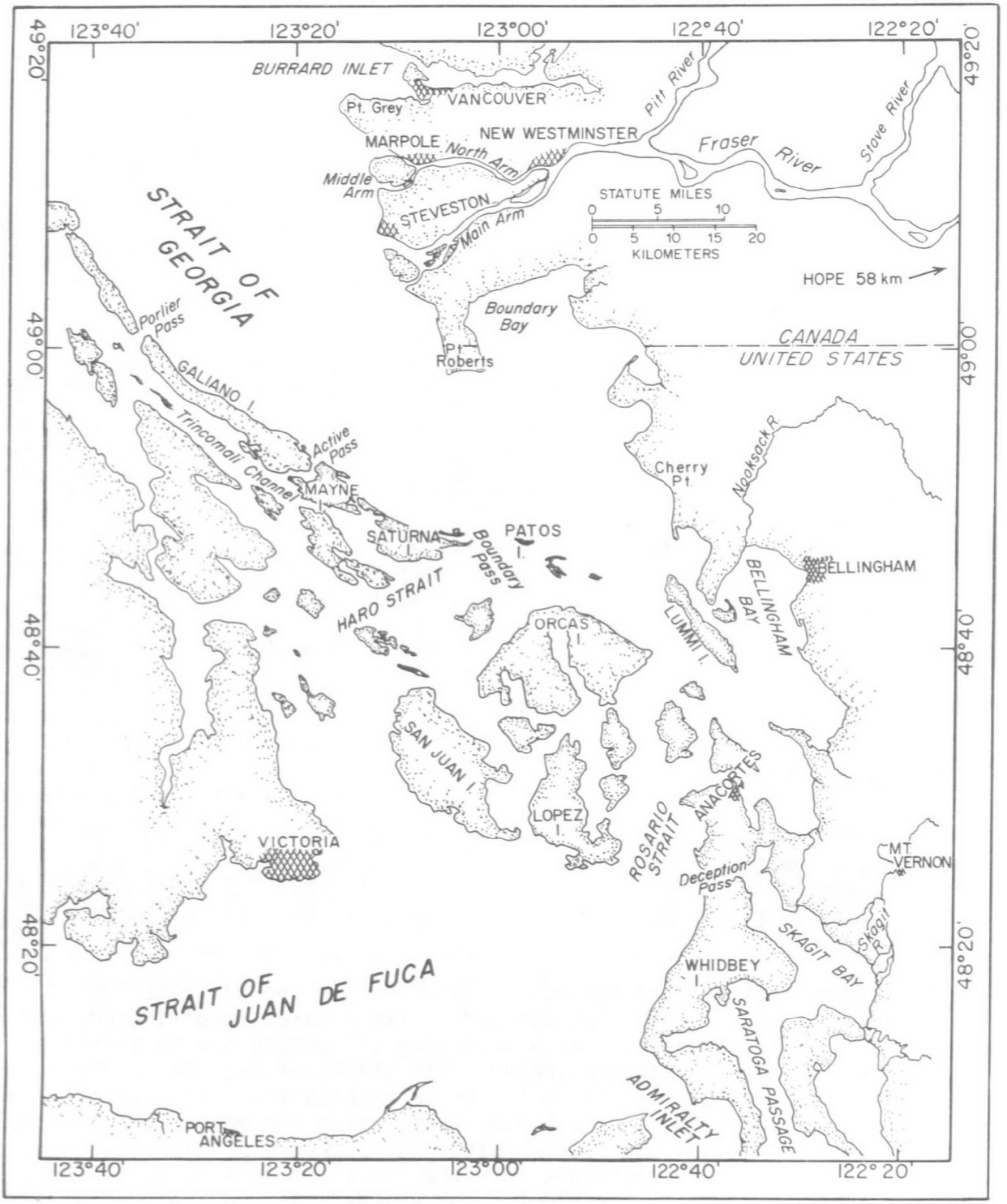

Figure 2.1 Physical setting of the study region

moves eastward through the strait, then northward through the San Juan passages, where it mixes with the less saline water of the Strait of Georgia.

Throughout most of the region the density structure of the water column is dominated by variations in salinity rather than in temperature. For example, during the summer months, the thermocline coincides with the halocline in the Strait of Juan de Fuca. However, in winter the waters are nearly isothermal and the stability is directly dependent upon the salinity structure. In the Strait of Georgia, tides and winds are the major controlling factors for mixing of surface waters, particularly in winter when nearly homogenous conditions prevail.

The influence of winds on surface circulation appears to be seasonally dependent. During the winter months the Aleutian Low determines the prevailing wind pattern for the Pacific Northwest, including British Columbia and Washington. The prevailing winds are predominantly from the southeast. In the Strait of Georgia the southeasterly winds set up a counterclockwise wind pattern over the area, providing energy to the surface waters and adding to the general counterclockwise circulation pattern. In the Strait of Juan de Fuca, west of Port Angeles, the orographic effect of the Olympic Mountains turns these winds seaward along the Strait. Wind speeds in this region average just over 20 knots. The surface waters respond to the wind forcing by absorbing energy from the winds and increasing surface currents in the general direction of the winds.

During the summer the North Pacific High predominates and the winds are primarily from the northwest. These winds are less intense and more variable; and, consequently, their effect on circulation of surface waters in the study area is less pronounced than in winter.

2.3 RIVER RUNOFF AND SEDIMENT DISCHARGE

Table 2.1 shows runoff data for the major rivers that discharge into the study region. The data show that of the total annual runoff, which is about 116 x $10^9 m^3$, greater than 90% is derived from two rivers, the Fraser River and the Skagit River.

The Fraser River drains an area of approximately 207,000 km^2, which consists of most of the Interior Plateau of British Columbia between the Coast Mountains and the Rocky Mountains. The elevated nature of the Interior Plateau determines the main feature of the discharge pattern which is the spring floods derived from melting snow. Figures 2.2a and 2.2b show the range, mean, and standard deviation of the water and sediment discharge at Hope, B.C., for the period between 1967 and 1977 (Water Survey of Canada, 1967-1977). The annual mean flow is 2960 cubic meters per second and the total annual sediment discharge is approximately 18 million metric tons (Table 2.2). The maximum discharge of water and suspended sediments occurs during the months of April through August.

TABLE 2.1 Average annual runoff from the major rivers discharging into the study region

River	Area of Drainage Basin (km^2)	Average Annual Runoff ($m^3 \times 10^9$)
Fraser*	207,000	93.4
Skagit**	8,040	14.2
Nooksack**	3,270	4.6
Stillaguamish**	1,790	3.6

*Water Survey of Canada, Water Data, Canadian Rivers, Inland Waters Directorate, Ottawa, Canada, 1967-1977.

**Pacific Northwest River Basins Commission. Puget Sound Task Force. Comprehensive Study of Water and Related Land Resources, Puget Sound and Adjacent Waters, State of Washington, Appendix III, Hydrology and Natural Environment, March 1970.

TABLE 2.2 Comparison of mean water and sediment discharge for the Fraser and Skagit Rivers during period of record (1967-1977)

Discharge Year	Fraser River at Hope**		Skagit River at Mt. Vernon***	
	River Discharge (m^3/sec)	Sediment Discharge (metric tons/day)	River Discharge (m^3/sec)	Sediment Discharge (metric tons/day)
1977	2589	36901	393	5670*
1976	3674	86560	497	1907
1975	2649	32683	561	2184
1974	3172	63428	596	3075
1973	2492	44043	379	-
1972	3398	79424	625	-
1971	2832	44544	551	-
1970	2166	32846	379	-
1969	2753	36032	414	-
1968	3313	64362	583	-
1967	3172	64139	464	-
Mean	2928	53178	495	3209
Std. Dev.	452	19245	93	1715

*January thru September.
**Water Survey of Canada (1967-1977).
***Water Resources Data for Washington, 1967-1977.

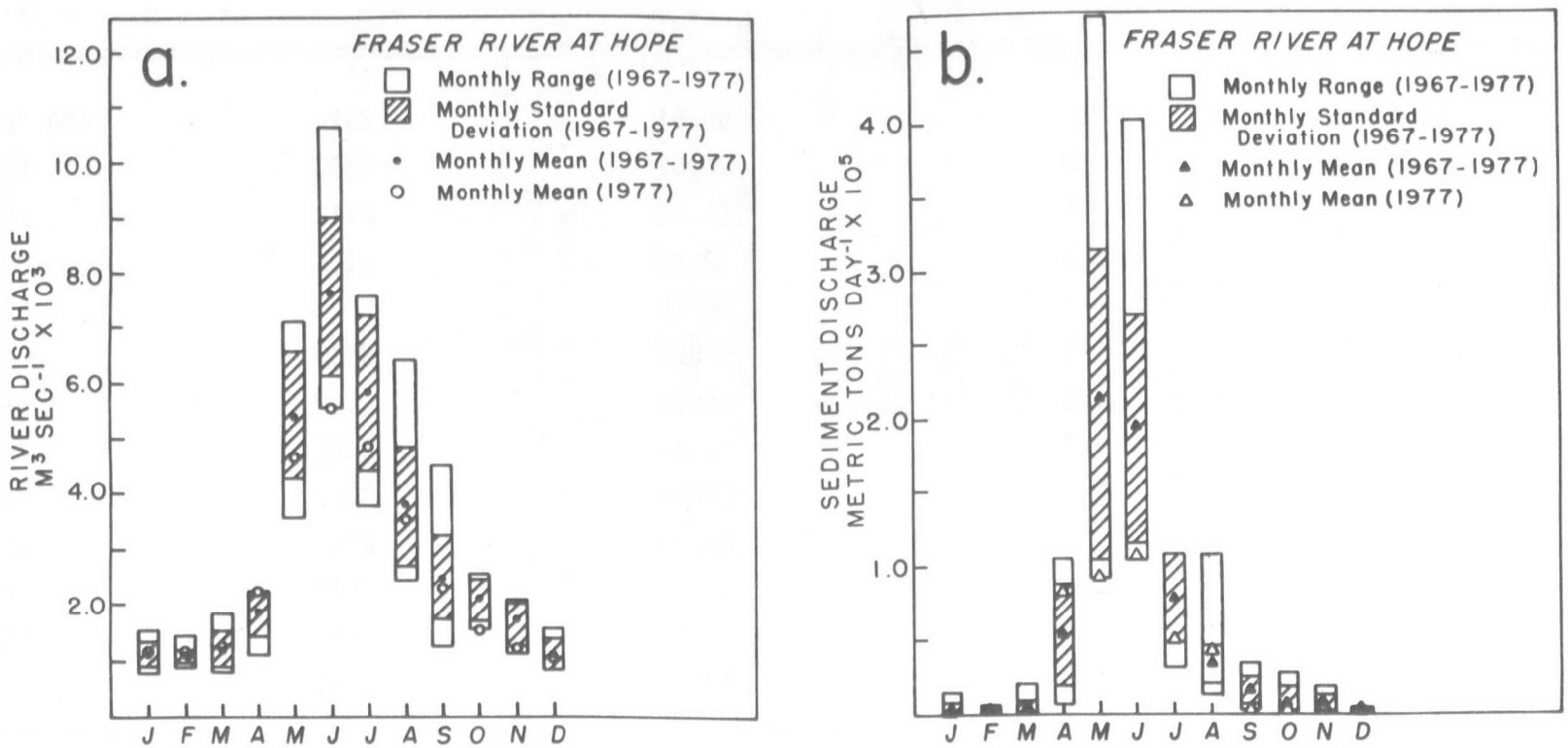

Figure 2.2 Monthly range, mean, and standard deviation of: a. water discharge; and b. suspended sediment discharge for the Fraser River at Hope, B.C. for the period from 1967 through 1977 (Water Survey of Canada, Sediment Data, Canadian Rivers, Inland Waters Directorate, Ottawa, Canada, 1967-1977).

At Hope, the Fraser River emerges from the Coast Mountains and flows through an alluvial valley to the Strait of Georgia. Near New Westminister (see Fig. 2.1), the Fraser bifurcates into a major channel or the Main Arm, which accounts for approximately 90% of the flow, and a minor channel, known as North Arm, which branches off at Marpole forming Middle Arm. Main Arm discharges into the Strait of Georgia at Stevenston and North Arm enters the Strait at Point Grey.

The Skagit River and its tributaries drain an area of approximately 8,040 km^2. The major tributaries of the Skagit River are the Baker, Cascade, and Sauk Rivers. The headwaters of the Skagit River and its tributaries are located in the North Cascade Range, where flow is partially derived from melting snow. Near Marblemount, Washington, the Skagit River is joined by the Cascade River, where it flows through broad flood plains and lowland areas until it reaches the coast. At a location about 12 km from the coast, the river splits into three distributaries which flow into Skagit Bay. Figure 2.3 shows water and sediment discharge data for the Skagit River at Mt. Vernon, Washington for 1975.* The data show a bimodal distribution for both water and suspended sediments. The major peaks occur in two periods: October through December and May through July. The October-December peak is associated with excessive rainfall in the lowland areas. The May-July peak corresponds with spring runoff due to melting snow near the headwaters.

---

*While water discharge records for the Skagit River are fairly complete from 1930 to the present, very few records for suspended sediments are available. Therefore, the records for 1975 were used to show the salient features of the Skagit River discharge pattern.

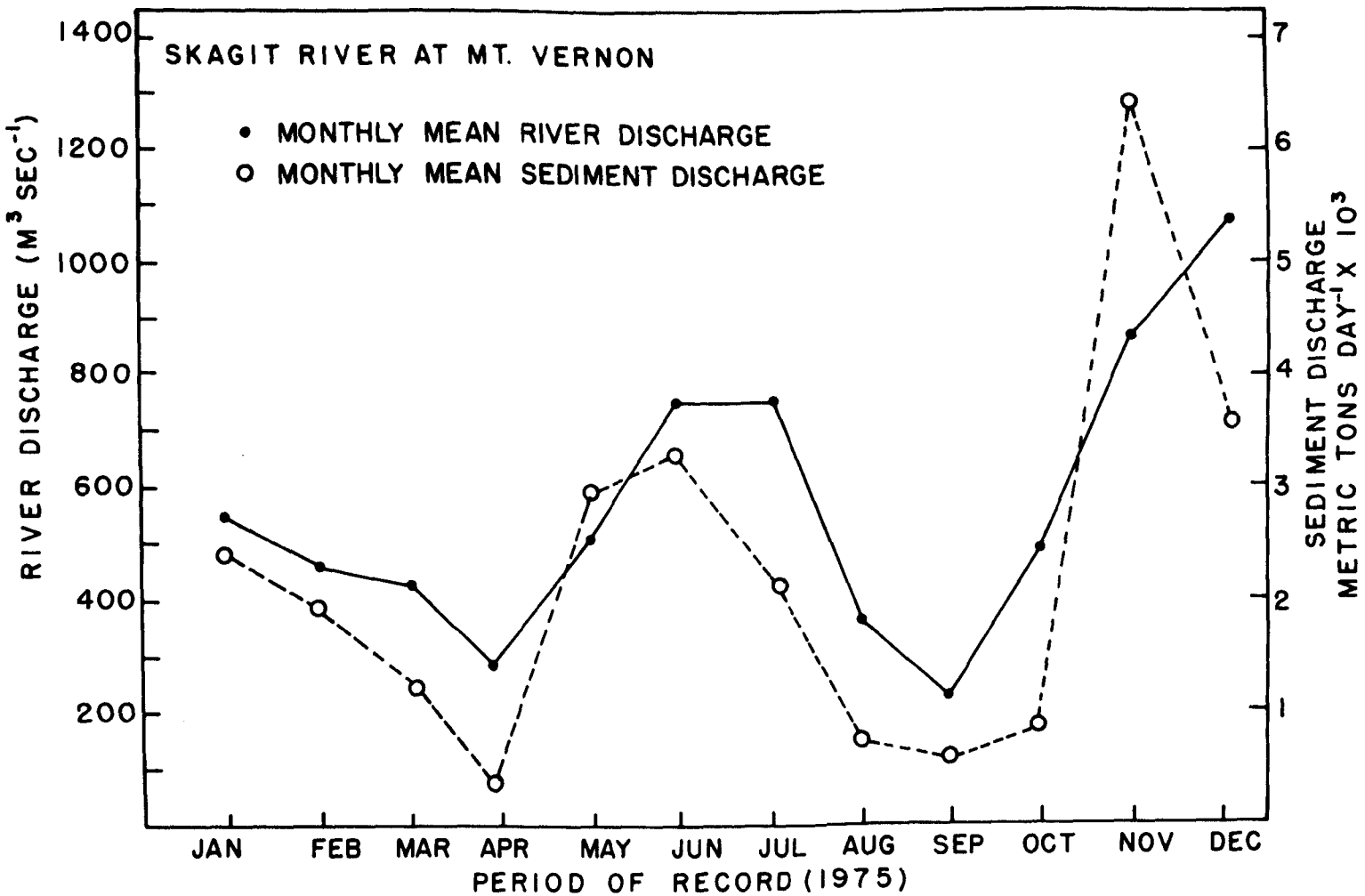

Figure 2.3 Monthly mean discharge of water and suspended sediments of the Skagit River at Mt. Vernon during 1975 (Water Resources Data for Washington, 1976).

3. CONCLUSIONS

3.1 LANDSAT IMAGERY

A set of LANDSAT images, obtained during the period between 1972 and 1978, have been utilized to study the surface trajectories of sediment plumes originating from the Fraser and Skagit Rivers. These plumes are natural tracers of the flow patterns of river water that are discharged into northern Puget Sound from these rivers.

Three separate plumes can be observed emanating from the mouths of the distributaries of the Fraser River. The plumes from Main Arm and Middle Arm join together to form a well-defined jet which can be traced across the Strait of Georgia and through Porlier, Active, and Boundary Passes. During ebb tide the plume is directed to the southeast from a point about midway between Steveston and Porlier Pass. The flood tide drives the plume across the Strait and to the northwest along the northern coast of Galiano Island.

The plume from North Arm moves to the northwest past Point Grey where it bifurcates, with some material flowing to the northwest during ebb tide and the remaining material moving into Burrard Inlet.

The existence of a number of separate plumes in some of the images suggests that the plumes are probably capable of maintaining their identity for periods longer than a single cycle. This implies that a dynamic balance exists between the inertial and pressure forces associated with the plumes and the coriolis and tidal forces associated with circulation patterns in the Strait.

The plumes from the distributaries of the Skagit River are most pronounced in early summer, during the peak runoff. During this period suspended sediments from the Skagit River can be traced as far south as the middle of Saratoga Passage and as far north as Deception Pass. During ebb tide, suspended solids from the Skagit River flow into Rosario Strait. During the period of low discharge, the Skagit River plume is confined to the nearshore regions of Skagit Bay.

3.2 QUANTITATIVE SEDIMENT MAPPING

A stepwise multiple linear regression analysis routine was employed to evaluate the relationships between the image radiance from the MSS Computer Compatible Tapes and sea-truth measurements of suspended matter concentrations. The results show that for the range of suspended matter concentrations observed in northern Puget Sound ($\approx$ 0.2 - 10.0 mg/l) MSS Band 5 radiance values, corrected for atmospheric interferences, are the most accurate for mapping suspended matter distributions. Consistent data, with relative errors on the order of 15-20%, can be obtained using relatively uncomplicated analytical procedures. The sediment distribution maps so generated are consistent with previously published data and provide greater detail than can be obtained with conventional sampling techniques.

4. RECOMMENDATIONS

Results of the present study indicate that the LANDSAT images are extremely useful for studying and mapping sediment plumes originating from the Fraser and Skagit Rivers. These data allow for synoptic observations of variations in plume trajectories which can be related to changes in the physical dynamics of the circulation patterns. In future studies of this kind, it may be more desirable to collect MSS data from high altitude airplanes rather than satellites. This would provide the kind of flexibility required to carry out more sophisticated field experiments.

5. METHODOLOGY

5.1 GENERAL STATEMENT

It is evident from the discussion in the introduction of this report that suspended materials, originating from the Fraser and Skagit Rivers, can play a major role in the dispersal and deposition of some fractions of crude oil and petroleum products that may be released as a result of oil transportation through the Strait of Georgia-Strait of Juan de Fuca system. Consequently, a comprehensive understanding of the dispersal mechanisms and trajectories of suspended matter from these rivers is essential to any model which attempts to predict the fates and potential impacts of oil in these waters. In recent years several advances in remote sensing techniques have allowed scientists to obtain synoptic information about water circulation and sediment dispersal patterns which heretofore have been unobtainable. The multispectral scanner images from the LANDSAT-1 and LANDSAT-2 satellites have been especially useful for the study of suspended matter transport processes in coastal and estuarine waters (Kritkos et al., 1974; Klemas et al., 1974; Gatto, 1976; Klemas and Polis, 1977; and Johnson et al., 1977).

Table 5.1 shows the major characteristics of the LANDSAT satellites and multispectral scanner. The multispectral scanner has four spectral bands. The green band (0.5-0.6 μm) and the red band (0.6-0.7 μm) provide information about dispersal patterns of suspended matter from major source regions such as rivers, streams, and coastal outfalls. The far red band (0.7-0.8 μm) only shows the core of the sediment plume and the near infrared band (0.8-1.1 μm) shows the shoreline. The data from the multispectral scanner is transmitted to a receiving station and then is converted to a photographic product.

5.2 LANDSAT IMAGERY AND HYDROGRAPHIC DATA

In order to provide synoptic information about variations of suspended matter dispersal patterns, water trajectories, and tidal mixing patterns, all clear (10% cloud cover or less) LANDSAT imagery from 1972 to the present were collected and correlated with corresponding data on water and sediment discharge (U.S. Geological Survey and Water Survey of Canada), water circulation (appropriate published literature as cited), and tides and tidal currents (Tide Tables, National Ocean Survey). LANDSAT photographs (MSS bands 4 and 5) were found to be ideal for studying the dispersal of turbid water. The sediment plumes, which appear lighter in tone than less turbid water in the images, are natural tracers of the low salinity water that exists offshore from the Fraser and Skagit River estuaries. However, the LANDSAT imagery only provides information about the upper few meters of the water column. Fortunately, previous studies have shown that the brackish water is generally confined to the upper 5 meters or less (Waldichuk, 1957; Tabata, 1972; and Schumacher et al., 1978) and, therefore, the LANDSAT imagery can be used to study the migration patterns of the low salinity water provided the sediment loading is sufficiently higher than the surrounding water.

TABLE 5.1 Principal characteristics of the LANDSAT satellite and multispectral scanner

System Parameters	Specifications
Satellite	
Altitude	915 km
Type of Orbit	circular, sun synchronous
Orbits per Day	14
Coverage Cycle	18 days
Time of Observation	approx. 1000 a.m. at 50° north latitude
Size of Area Imaged	185 x 185 km
Field of View	11.56°
Side Lap	67%
Overlap Along Orbit	10%
Multispectral Scanner	
Image Distortion	2%
Ground Resolution	80 to 120 meters
Position Accuracy	900 meters
Spectral Bands, Bandwidths (μm), and Nominal Color	4: 0.5-0.6; green 5: 0.6-0.7; red 6: 0.7-0.8; far red 7: 0.8-1.1; near infrared

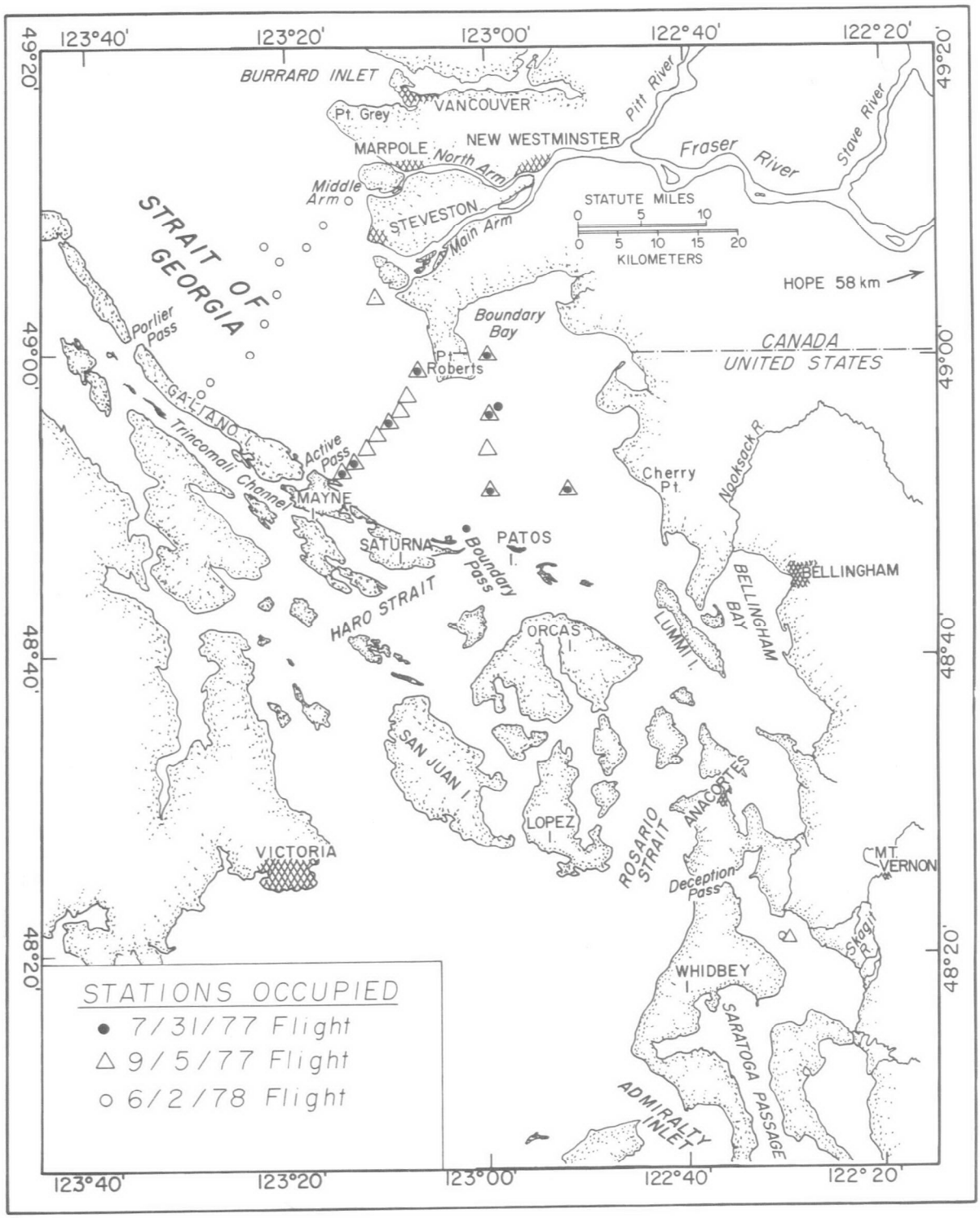

Figure 5.1 Locations of sampling stations for sea truth measurements.

5.3 SEA-TRUTH MEASUREMENTS

On three separate occasions (July 31 and September 5, 1977 and June 2, 1978) a Cessna 206 seaplane was employed to collect surface water samples at approximately the same time of day as the satellite overpasses (Fig. 5.1). Water samples were collected in acid cleaned 1-l polyethylene bottles held approximately 5-10 cm below the air-seawater interface. The samples were returned to the laboratory and within 9 hours were filtered through pre-weighed 0.4 μm pore size 47 mm Nuclepore filters. The filters were washed with three 15 ml aliquots of deionized membrane filtered water, dried in a desiccator and reweighed on a Cahn Electrobalance. The samples were then treated with 15% H_2O_2 to remove oxidizable organic matter (Baker, 1973), dried in a desiccator and weighed again.

5.4 MSS COMPUTER COMPATIBLE TAPES

MSS Computer Compatible Tapes of the LANDSAT images, which were supplied by the EROS Data Center, Sioux Falls, S.D., were processed in the following manner. Sample locations were found on the photographic images from which pixel coordinates were determined and using those coordinates, radiance values in the four multispectral bands were recalled from the MSS computer tapes. Average radiance values for a 7 x 7 pixel field corresponding to the sample points were then determined, and atmospheric corrections were applied to the previous data by determining the radiance values of clear water and subtracting them from each of the measured radiance values. Finally, step-wise multiple linear regression techniques were employed to quantitatively relate the remotely sensed data to the sea-truth measurements.

The atmospheric correction just described assumes that atmospheric effects are constant over the entire area of interest and the resulting corrected radiance values are attributed to the suspended material in the water. This assumption is only true for regions which are free of cloud cover as suggested by the discussion of Bowker and Witte (1975). Therefore, the atmospheric corrections discussed in the following sections of this report have only been applied to specific scenes where cloud cover is limited to areas which do not affect the integrity of the data.

6. RESULTS AND DISCUSSION

6.1 SEASONAL VARIATIONS OF SEDIMENT DISPERSAL

The amount of useful information about seasonal variations of suspended sediment distributions and dispersal patterns that can be obtained from LANDSAT imagery is somewhat limited because most cloud-free days occur during the summer; and, as a result, the majority of available images are from that season. However, two high quality images* from January 1973 (Figs. 6.1 and 6.2) and one from March 1976 (Fig. 6.3) are available. Therefore, some general statements about sediment dispersal patterns for winter, spring, and summer can be made.

When the fresh water and sediment discharge from the Fraser River are high, particularly during the spring floods and during the ebbing tide, the longitudinal pressure head at the river mouth produces a well-defined turbid plume which extends outward into the Strait of Georgia. The orientation of the plume axis can be used to determine the direction of flow. During the months of May through August, the southward flow of Main Arm and Middle Arm is so strong that the resultant plume maintains its identity for a considerable distance and, in some cases, traverses the entire length of the Strait. Figures 6.4, 6.6, and 6.9 are examples of this phenomenon. Depending upon local changes in tidal currents, the plumes extend either to the southeast or southwest from the river mouth. Tidal mixing is rapid and numerous eddies are apparent.

At the mouths of Middle Arm and North Arm there was some evidence of flow to the northwest in most of the images. This feature is particularly evident in Figures 6.6 and 6.7. These plumes appear to maintain their identity as far north as Point Grey and the entrance to Burrard Inlet.

The Skagit River plume flows into Skagit Bay and Saratoga Passage during the summer months (Figs. 6.4 thru 6.9). Some plume material passes through Deception Pass into Rosario Strait during ebb tide (Fig. 6.8).

The winter plumes from the Fraser and Skagit Rivers, as shown in the LANDSAT images from January 1973 and March 1976 (Figs. 6.1 thru 6.3), are much less distinct than that observed during summer. For instance, the Fraser River plumes in January and March are only visible in the nearshore regions just a few kilometers seaward of the river mouth, where the primary flow pattern is to the southeast. During this period, the discharge of both water and suspended sediments are at a minimum. Average discharge rates for water and sediments are approximately 10-30% of the mean annual rates (see Fig. 2.2). This means that both the longitudinal pressure gradient and the suspended sediment concentrations are greatly reduced in winter. Consequently,

---

*Specific characteristics of the images are uniquely identified in the figures by numbered markers and are described both in the text and in the figure captions.

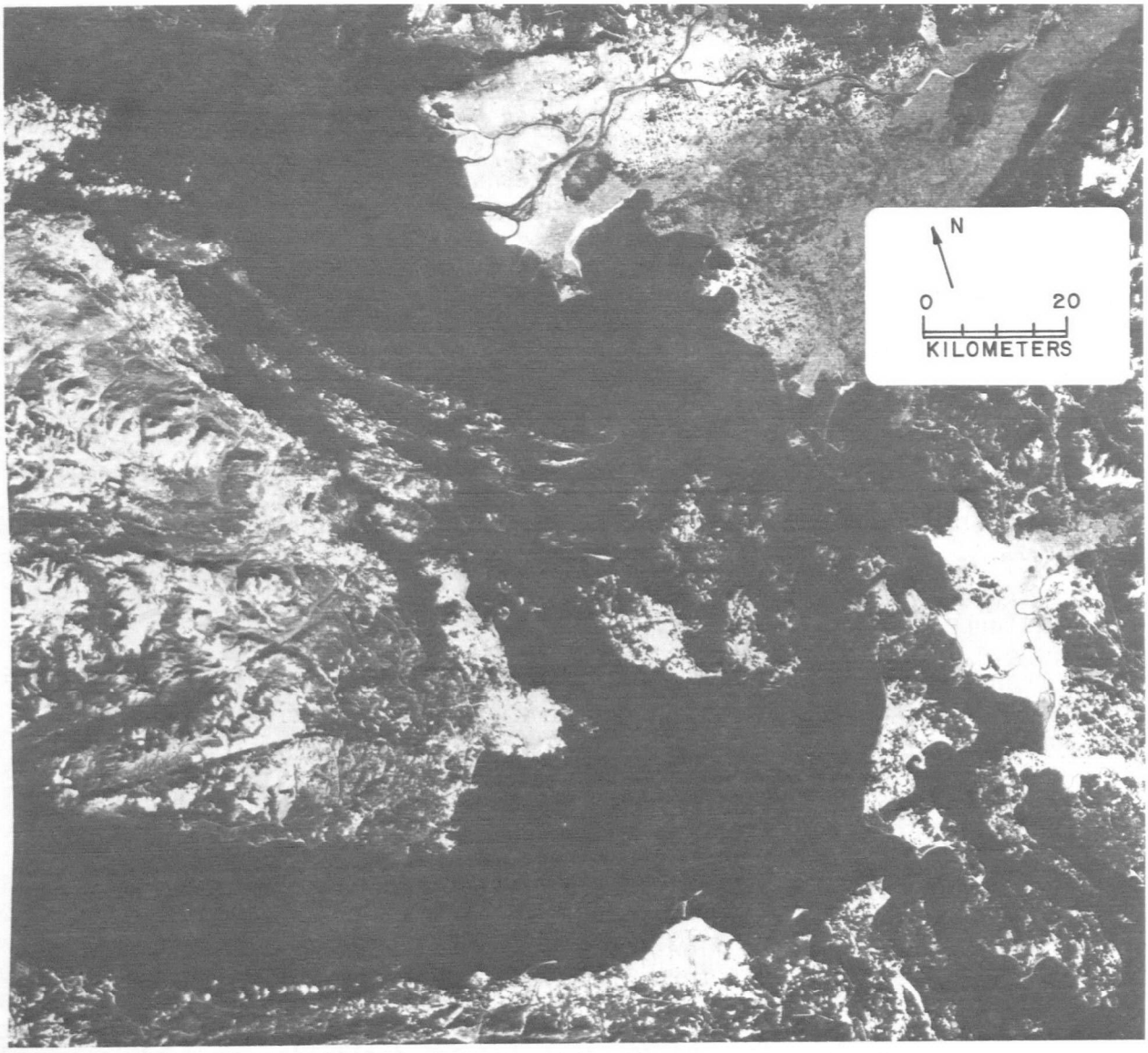

Fig. 6.1 MSS Band 5 of LANDSAT image 1169-18373 on Jan. 8, 1973 between slack water and minor ebb current. Time of image acquisition was 1037 PST. The image shows little evidence of sediment dispersal from the Fraser River into the Strait of Georgia, reflecting the lower water and sediment discharge during the winter season. The image is free of cloud cover.

TIDAL CURRENT:			TIDES:		WINDS:
Slack Water	Max. Current	Vel. (kts)	Time	Ht.(m)	Time of image SE @ 1.6 kms/hr
	0515	1.7	High @ 0834	2.9	12 hrs earlier E @ 4.8 kms/hr
0906	1209	1.7	Low @ 1429	1.6	24 hrs earlier E @ 19 kms/hr

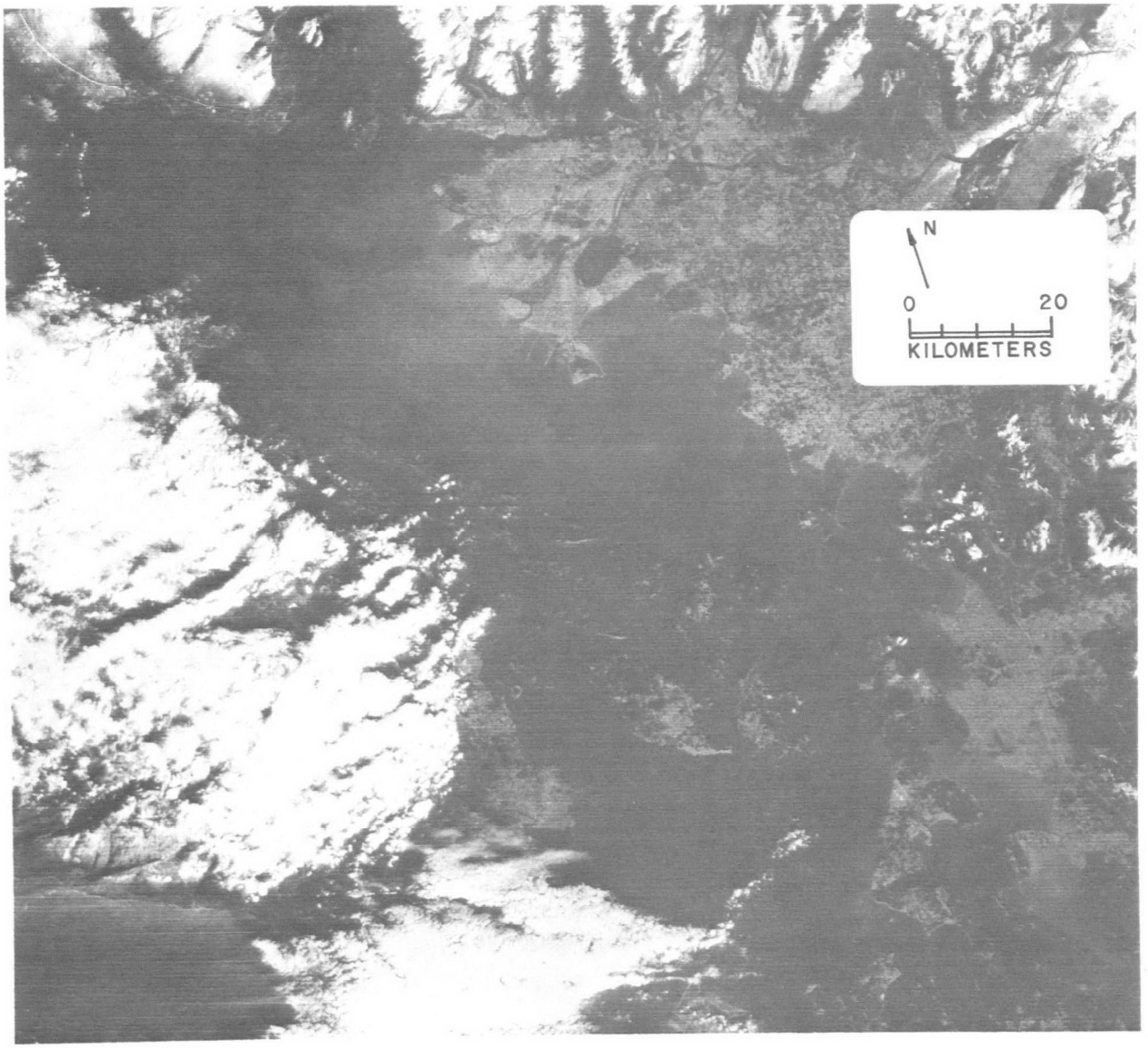

Fig. 6.2 MSS Band 5 of LANDSAT image 1187-18374 on Jan. 26, 1973. Time of image acquisition was 1037 PST, between slack water and major ebb current. The image shows limited dispersal of suspended sediments into the Strait of Georgia from the Fraser River.

TIDAL CURRENT:

Slack Water	Max. Current	Vel. (kts)
0508	0733	0.9
1008	1501	2.3

TIDES:

Time	Ht.(m)
High @ 0905	2.6
Low @ 1811	0.4

WINDS:

Time of image E @ 12.8 kms/hr
12 hrs earlier E @ 9 kms/hr
24 hrs earlier W @ 24 kms/hr

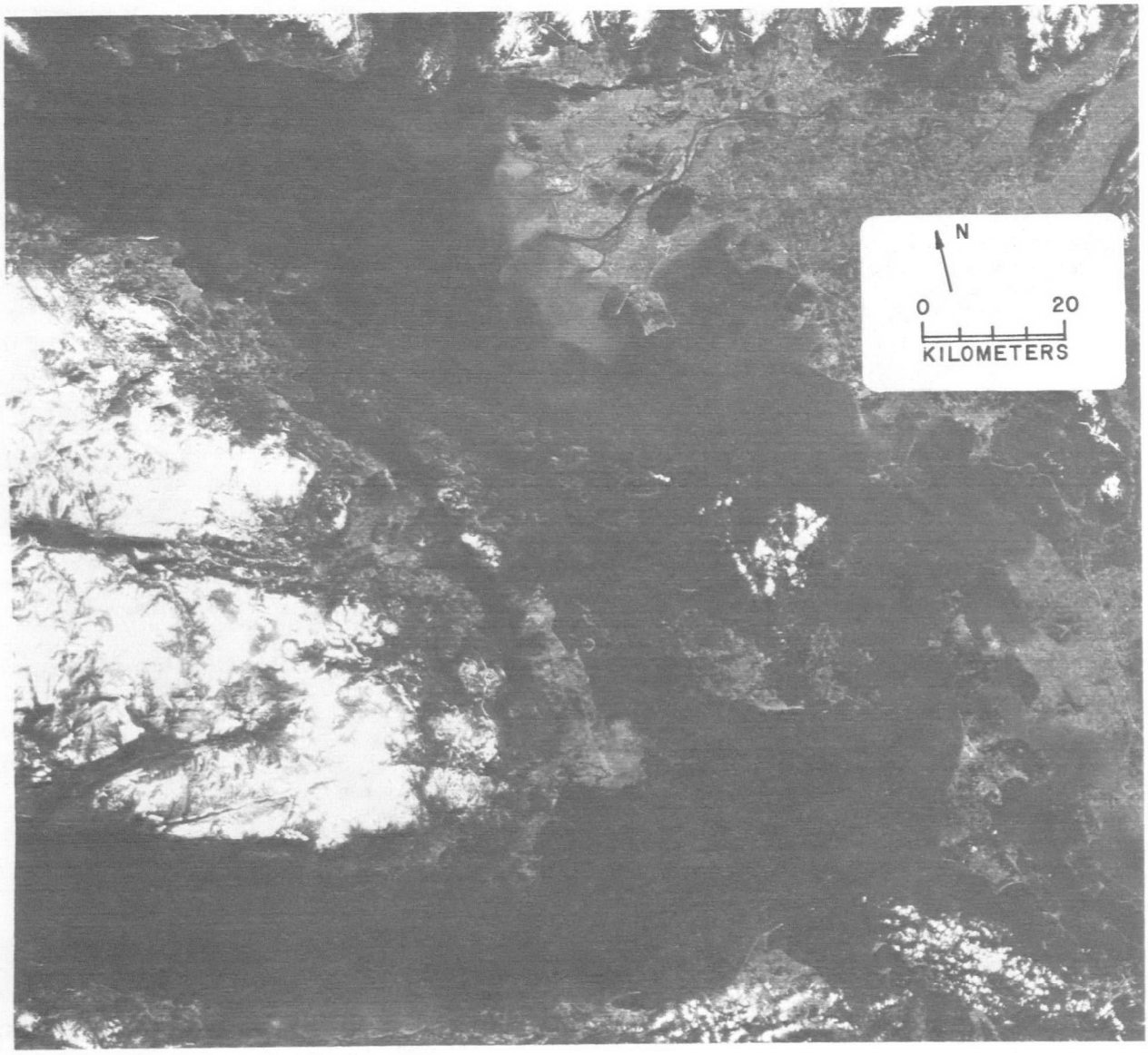

Fig. 6.3 MSS Band 4 of LANDSAT image 2417-18220 on Mar. 14, 1976. Time of image acquisition was 1022 PST, between minor ebb current and slack water. The image shows limited dispersal of suspended sediments into the nearshore waters south and southeast of the mouths of Main, Middle and North Arms.

TIDAL CURRENT:

Slack Water	Max. Current	Vel. (kts)
0454	0806	1.8
1150	1322	0.8

TIDES:

Time	Ht.(m)	Time of image NW @ 37 kms/hr
Low @ 0808	0.8	12 hrs earlier NW @ 19 kms/hr
High @ 1402	1.9	24 hrs earlier NW @ 3.2 kms/hr

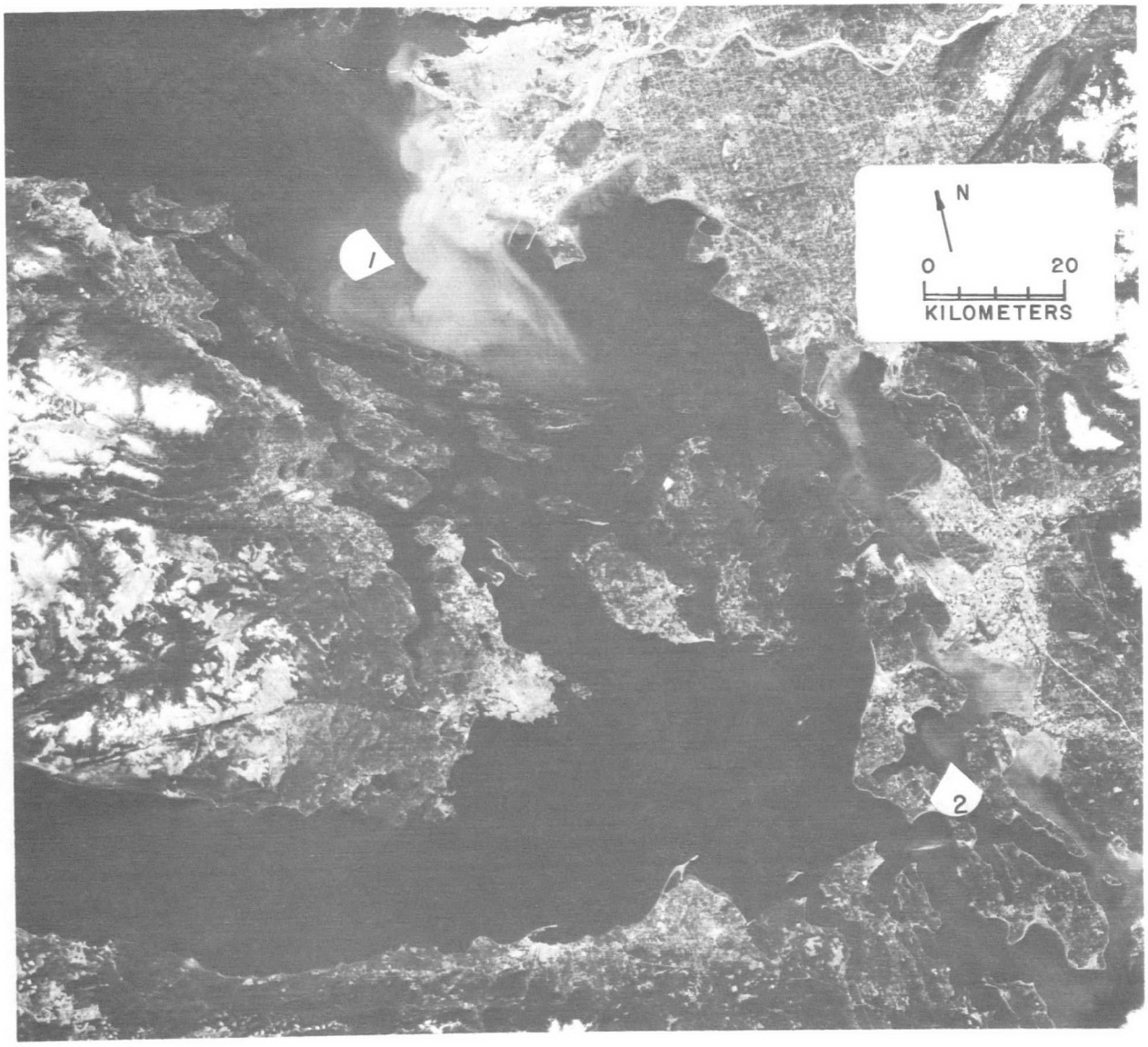

Fig. 6.4 MSS Band 5 of LANDSAT image 2111-18254 showing a southeasterly dispersal (1) of suspended sediments from the Fraser River into the Strait of Georgia on May 13, 1975. Time of image acquisition was 1025 PST, between major ebb current and slack water. The dispersal pattern shows movement of Fraser River sediments into Haro Strait, primarily through Boundary Pass. Sediment discharge from the Skagit River into Skagit Bay and Saratoga Passage is evident (2).

TIDAL CURRENT:

Slack Water	Max. Current	Vel. (kts)
0506	1000	2.9
1404	1643	2.4

TIDES:

Time	Ht.(m)
High @ 0449	2.4
Low @ 1246	-0.5

WINDS:

Time of image NW @ 32 kms/hr
12 hrs earlier N @ 6 kms/hr
24 hrs earlier SE @ 12.8 kms/hr

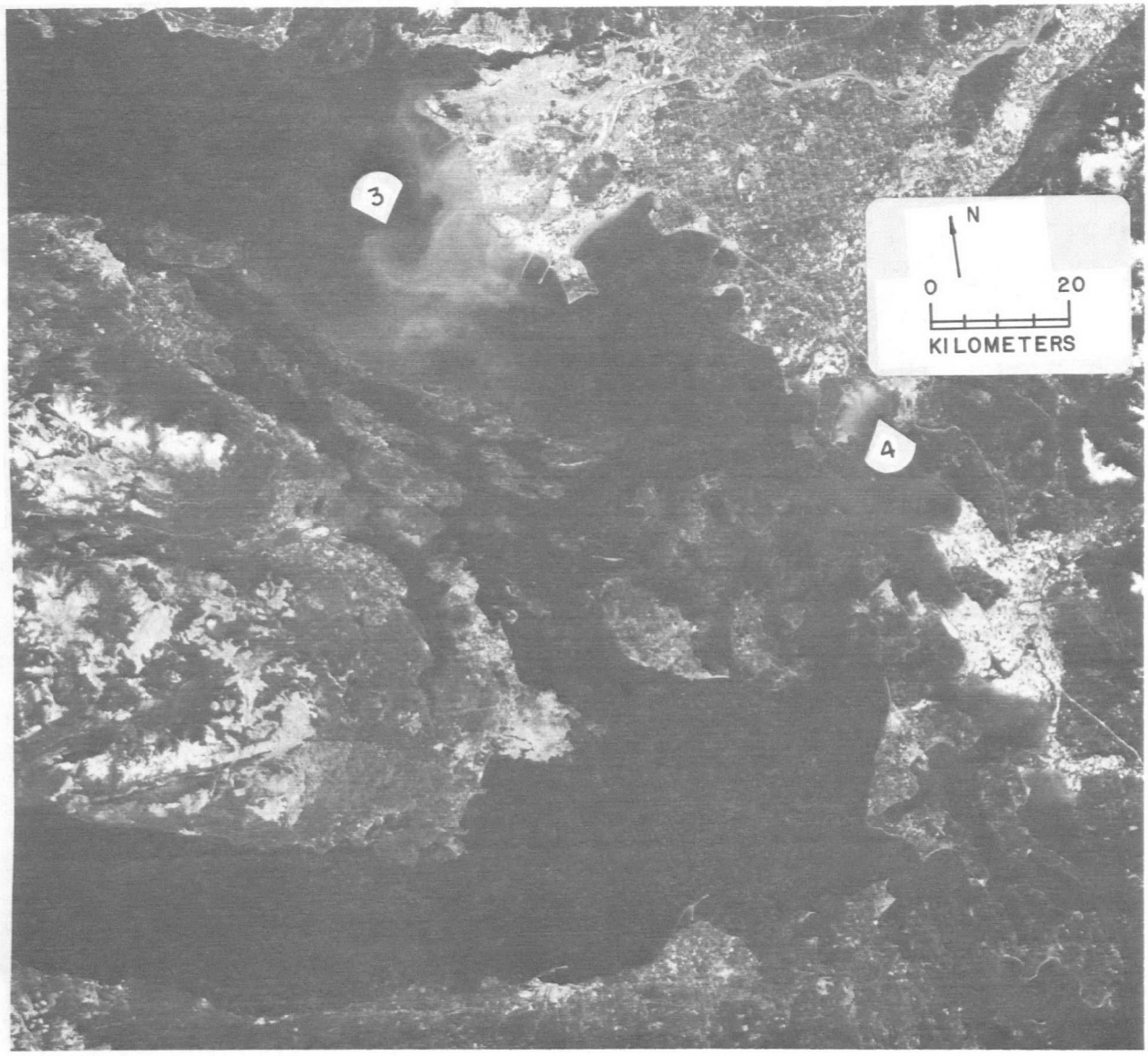

Fig. 6.5 MSS Band 5 of LANDSAT image 2129-18254 showing a southwesterly dispersal of suspended sediments from the Fraser River into the Strait of Georgia on May 31, 1975. Time of image acquisition was 1025 PST, just after flood current. An anticyclonic gyre can be observed due west of Pt. Roberts (3). Sediment discharge from the Nooksack River can be seen in Bellingham Bay (4). Image is free of cloud cover.

TIDAL CURRENT:			TIDES:		
Slack Water	Max. Current	Vel. (kts)	Time	Ht.(m)	Time of image NW @ 17 kms/hr
	0650	weak and variable	High @ 0821	1.7	12 hrs earlier SW @ 4.8 kms/hr
	1256	1.6	Low @ 1522	0.3	24 hrs earlier NW @ 14 kms/hr

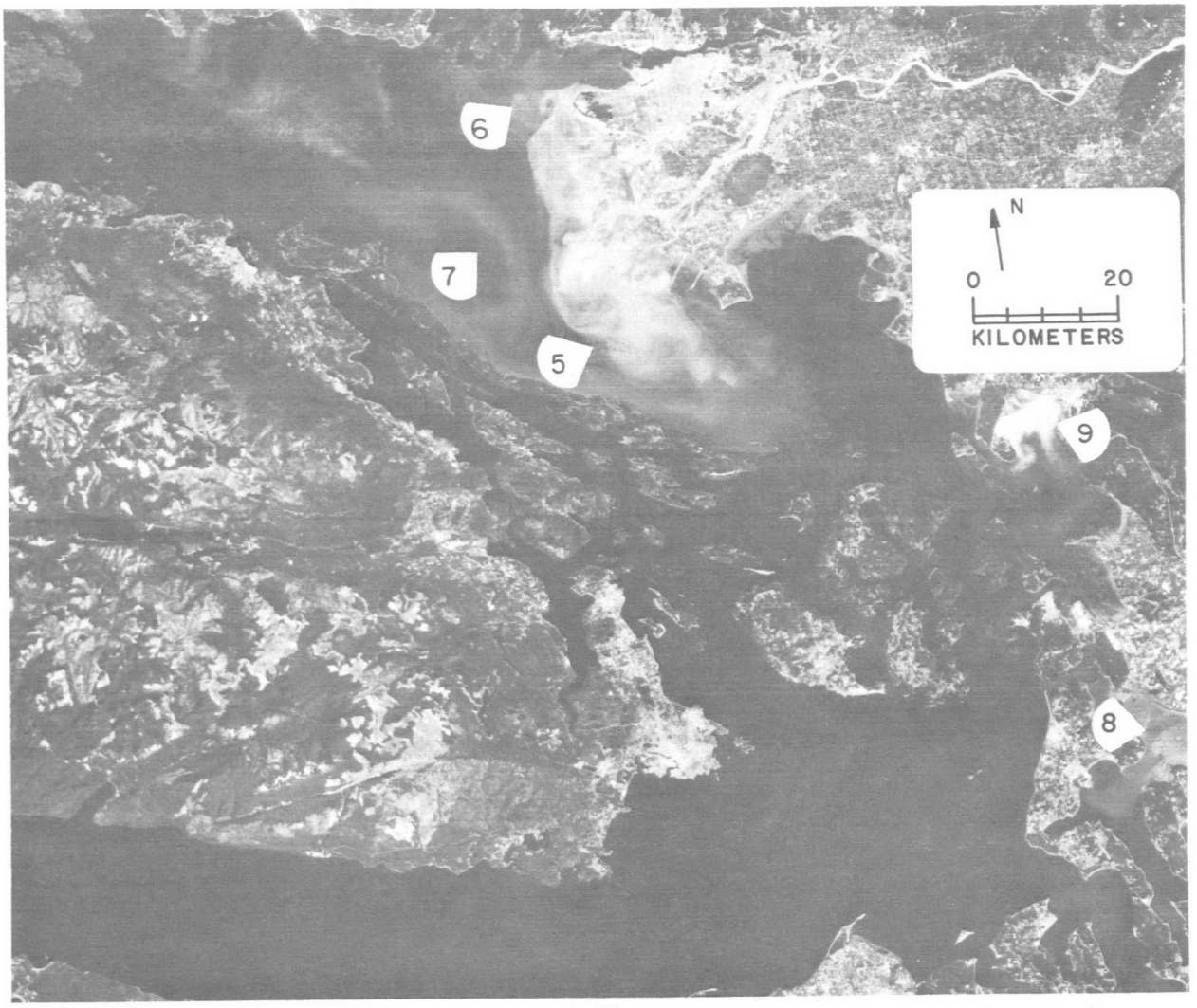

Fig. 6.6 MSS Band 5 of LANDSAT image 1727-18290 showing a southeasterly dispersal (5) of suspended sediments from the Fraser River into the Strait of Georgia on July 20, 1974. Time of image acquisition was 1029 PST, between major ebb current and slack water. The dispersal pattern suggests movement of Fraser River sediments along Saturna, Mayne, and Galiano Islands and into Trincomali Channel from Porlier Pass. Suspended sediments from the North Arm appear to flow to the northwest and to the northeast into Burrard Inlet (6). A cyclonic eddy (7) can be observed north of Galiano Island. Sediment discharge from the Skagit River into Skagit Bay (8), and from the Nooksack River into Bellingham Bay (9) is clearly visible. Several tidal fronts are also observed in the Strait of Juan de Fuca.

TIDAL CURRENT:

Slack Water	Max. Current	Vel. (kts)
0429	0912	3.1
1303	1534	2.0

TIDES:

Time	Ht.(m)
Low @ 1147	-0.7
High @ 1904	2.7

WINDS:

Time of image SE @ 1.6 kms/hr
12 hrs earlier SW @ 1.6 kms/hr
24 hrs earlier SE @ 1.6 kms/hr

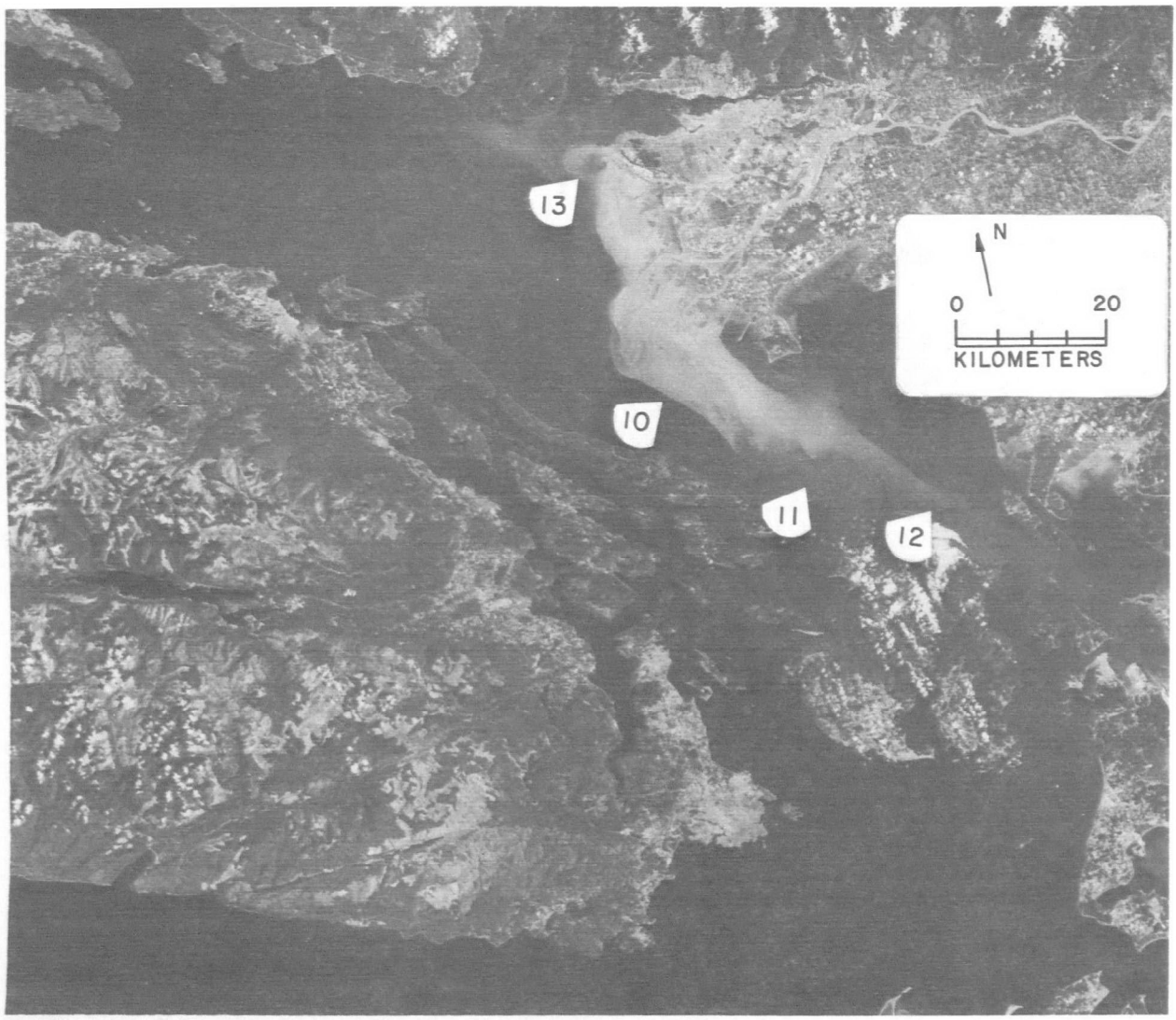

Fig. 6.7 MSS Band 5 of LANDSAT image 5465-17484 showing a southeasterly dispersal (10) of suspended sediments from the Fraser River into the Strait of Georgia on July 27, 1976. Time of image acquisition was 1048 PST, between major ebb current and slack water. The dispersal pattern suggests movement of Fraser River sediments into Haro Strait from the passages on either side of Mayne and Saturna Islands (11), and into Rosario Strait from the south-eastern Strait of Georgia (12). Suspended sediments discharging into the Strait from North Arm appear to flow northward past Pt. Grey where it bifurcates, a portion flowing to the northwest, and the remaining flowing to the northeast into Burrard Inlet (13).

TIDAL CURRENT:			TIDES:		WINDS:
Slack Water	Max. Current	Vel. (kts)	Time	Ht.(m)	Time of image NW @ 25 kms/hr
0408	0904	2.7	High @ 0225	1.9	12 hrs earlier W @ 48 kms/hr
1224	1517	1.8	Low @ 0931	-0.7	24 hrs earlier NW @ 21 kms/hr

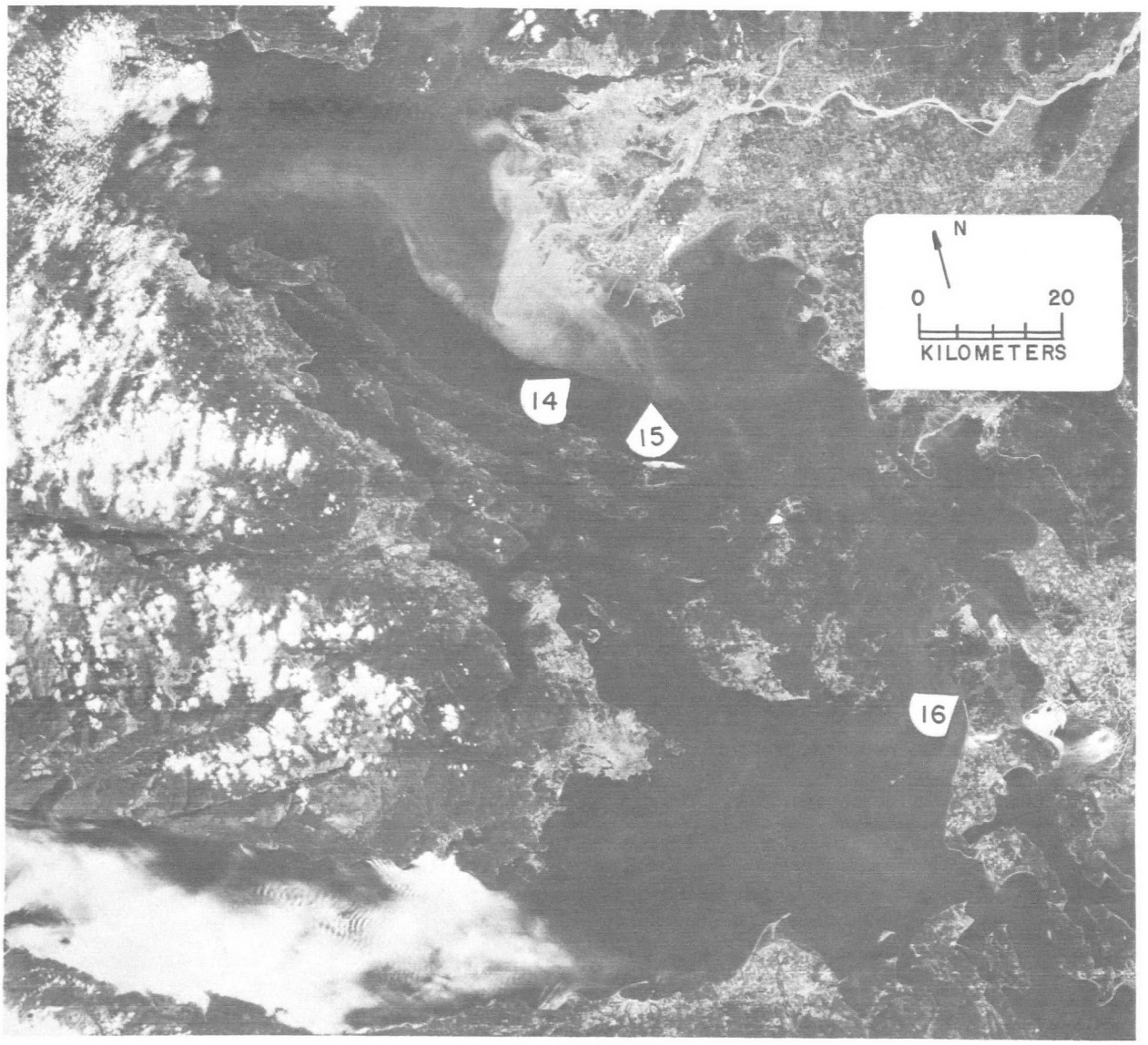

Fig. 6.8 MSS Band 4 of LANDSAT image 2921-18025 showing southeasterly dispersal (14) of suspended sediments from the Fraser River into the Strait of Georgia on July 31, 1977. Time of image acquisition was 1002 PST, between major ebb current and slack water. A density front is clearly indicated in the center of the Strait of Georgia (15). Suspended sediments can be observed discharging into Skagit Bay and through Deception Pass into Rosario Strait (16).

TIDAL CURRENT:			TIDES:		
Slack Water	Max. Current	Vel. (kts)	Time	Ht.(m)	Time of image NW 25 kms/hr
	0921	3.1	High @ 0437	2.4	12 hrs earlier S 1.6 kms/hr
1306	1531	1.8	Low @ 1149	-0.4	24 hrs earlier S 14 kms/hr

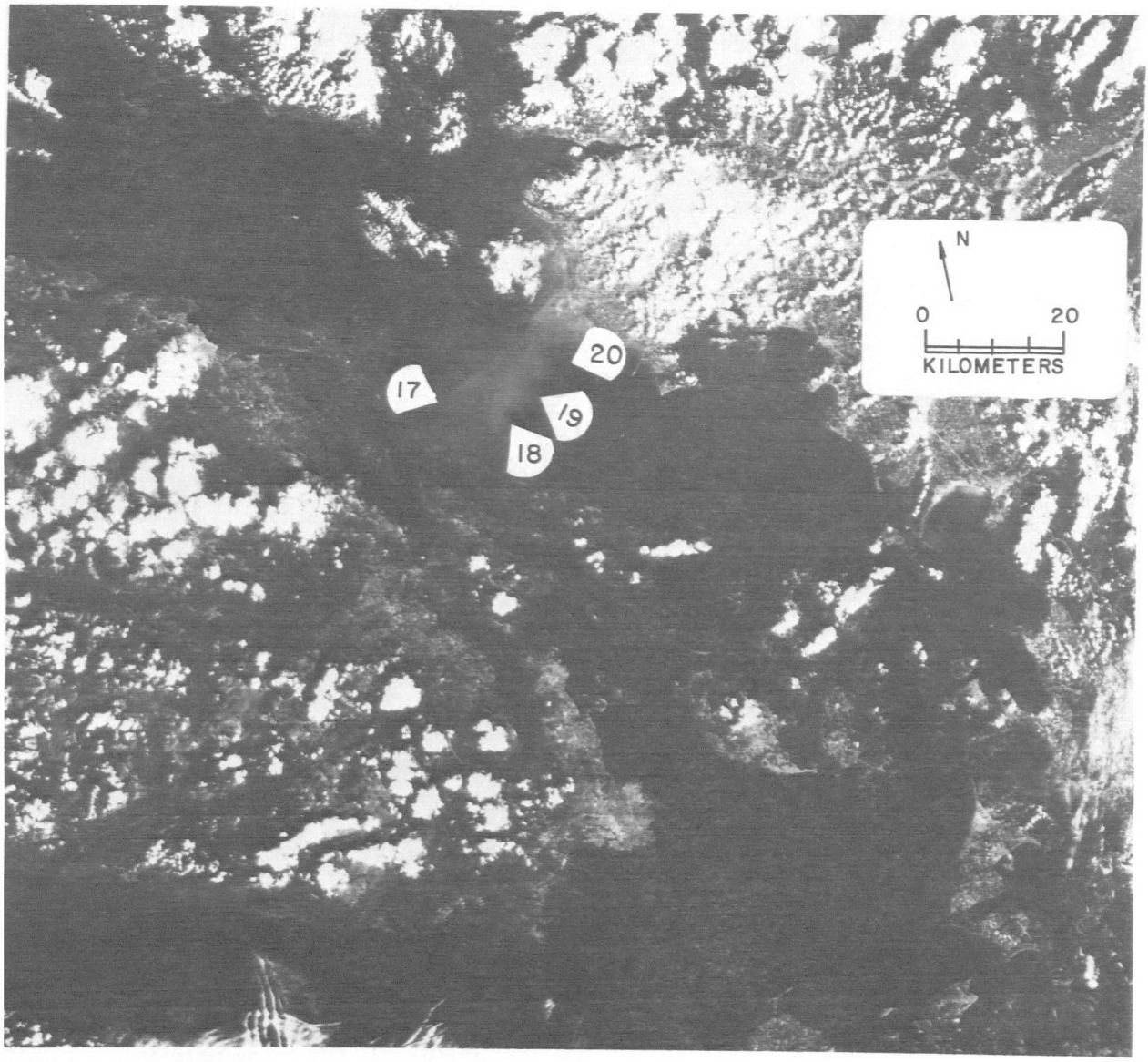

Fig. 6.9 MSS Band 5 of LANDSAT image 2957-18004 showing a southwesterly dispersal (17) of suspended sediments from the Fraser River into the Strait of Georgia on Sept. 5, 1977. Time of image acquisition was 1000 PST, between major flood current and slack water. The dispersal pattern suggests southwesterly flow associated with the flood current. Three small cyclonic eddies can be observed north of Mayne Island (18, 19 and 20). 40% cloud cover is visible over most land masses.

TIDAL CURRENT:			TIDES:		WINDS:
Slack Water	Max. Current	Vel. (kts)	Time	Ht.(m)	Time of image W @ 13 kms/hr
	0756	0.7	Low @ 0414	0.4	12 hrs earlier SW@ 14 kms/hr
1201	1502	0.7	High @ 1227	1.9	24 hrs earlier S @ 16 kms/hr

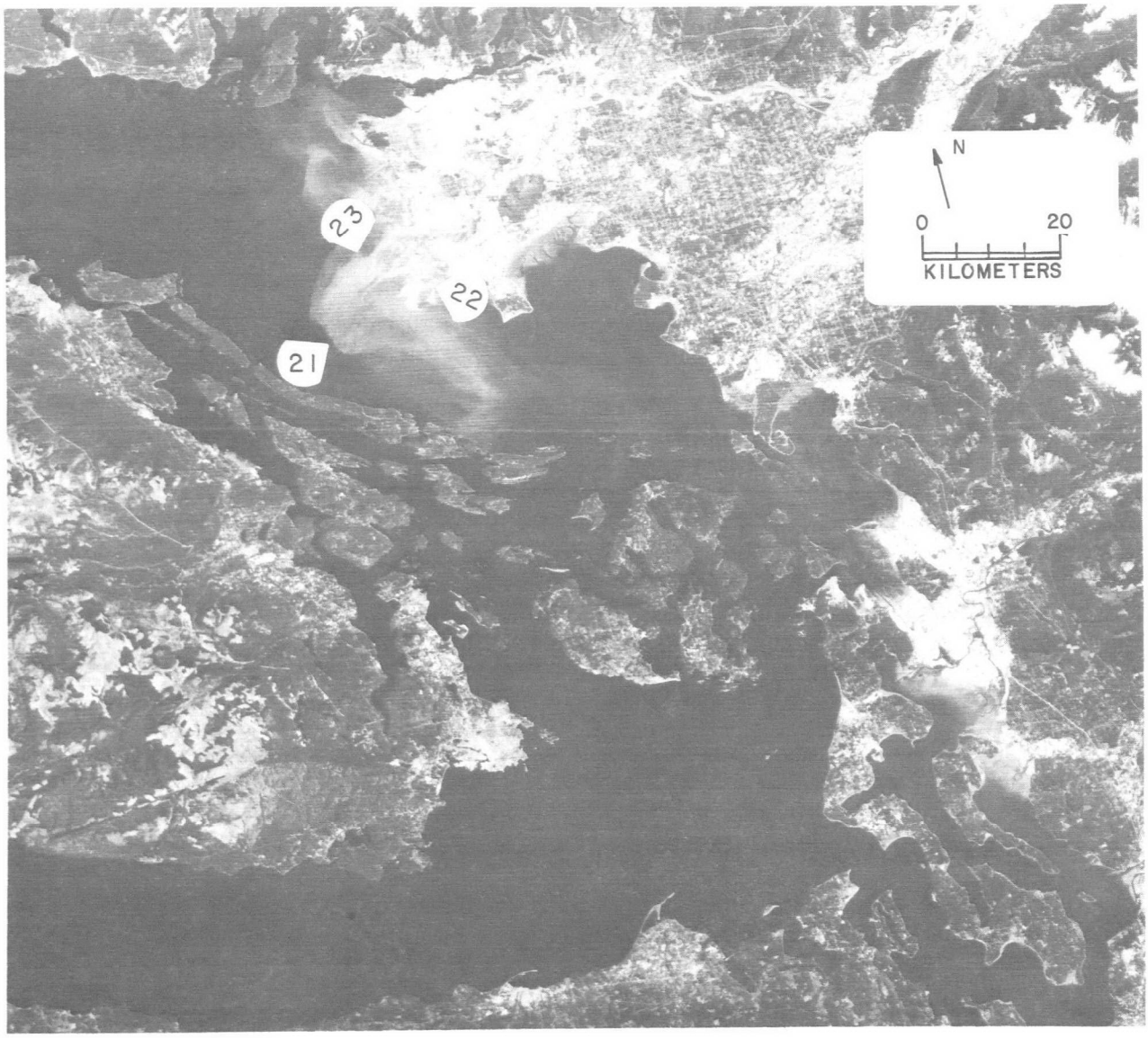

Fig. 6.10 MSS Band 5 of LANDSAT image 21227-18025 showing a southeasterly dispersal (21) from the Fraser River into the Strait of Georgia on June 2, 1978. Time of image acquisition was 1025 PST, shortly before slack water following major ebb current. Several definitive plumes of sediment laden water are observed coming from Main Arm (22 and 23). A density front can be seen in the center of the Strait of Georgia. Plumes are observed dispersing into Rosario Strait from the north side of Orcas Island.

TIDAL CURRENT:			TIDES:		WINDS:
Slack Water	Max. Current	Vel. (kts.)	Time	Ht.(m)	Time of image NW @ 19 kms/hr
	0630	2.8	Low @ 0945	0.1	12 hrs earlier NW @ 11 kms/hr
1050	1340	1.2	High @ 1623	2.2	24 hrs earlier N @ 11 kms/hr

the forces which drive the Fraser River plume into the Strait of Georgia are diminished in winter, resulting in more rapid mixing of the plume and concurrent dilution of suspended sediment concentrations to background levels. These conclusions are substantiated by the results of the seasonal surveys of suspended matter concentrations in the vicinity of the Fraser River which were presented in a previous report (Baker et al., 1978). The background concentration of suspended matter in the study region was found to be approximately 1.0 mg/l. Near the mouth of the Fraser River particulate concentrations ranged between 2.5 and 9.0 mg/l during the November and August surveys (see, for example, stations 25, 26, and 27 in Figs. 5.4 and 5.6 in Baker et al., 1978). However, in March the particulate concentration for station 25 was 0.9 mg/l or approximately the same as background values for this region and time of year, indicating rapid dilution of the Fraser River plume as it discharges into the Strait.

The Skagit River also shows a minimum in water and sediment discharge during the winter period (Fig. 2.3). However, the percentage decrease is not as large as the winter decrease of the Fraser River (the average water and sediment discharge rates for the Skagit River during the months of January through March are 50-70% of the mean annual rates); and, as a result, the seasonal variations of the Skagit River plume are not nearly as pronounced. The LANDSAT images for January 1973 and March 1976 show evidence for movement of suspended sediments from the Skagit River into the nearshore regions of Skagit Bay (Figs. 6.2 and 6.3). This material mixes rapidly with the offshore water and the plumes do not maintain their identity beyond Deception Pass.

6.2 TIDAL VARIATIONS OF SEDIMENT DISPERSAL

As indicated in Table 5.1, the LANDSAT satellites maintain a sunsynchronous orbit around the earth in such a manner as to arrive at the same location at approximately the same time of day once every 18 days. Because the average tidal interval is about 12 hours 25 minutes, the tides will be out of phase by approximately one quarter cycle each time the satellite passes over. This means that over the course of several years the LANDSAT imagery for a given location should include all tidal stages if proper atmospheric conditions have prevailed. Since their deployment in 1972 and 1975, the LANDSAT satellites have produced approximately nine or ten high quality images which can be used for describing tidal effects on the dispersion of the Fraser River plume.

Figures 6.3 through 6.10 show examples of LANDSAT imagery which are of sufficient quality to be useful for studying tidal processes. The ebb tides are represented by Figures 6.3, 6.4, 6.6, 6.7, 6.8, and 6.10 and flood tides are indicated in Figures 6.5 and 6.9. The tidal stage corresponding to each of the LANDSAT images has been determined and is included in the figure captions. Patos Island was used as a reference point for determination of the tidal stage because: (1) it is centrally located with respect to the northern part of the study region and, consequently, differences in tidal stages are relatively small (e.g., the tides at the mouth of Main Arm precede those at Patos Island by about 2-4 minutes, whereas the tides at Deception Pass precede those at Patos Island by about 77 minutes); and (2) it provided the most complete set of data on tides and tide currents.

During ebb tide, distinct sediment plumes originating from Main Arm and Middle Arm flow seaward in a southwesterly direction to a point approximately midway between Steveston and Porlier Pass where the plumes are diverted in a southeasterly direction by the ebb flow in the Strait. Figures 6.4, 6.6, and 6.7 are examples of this process. The sediment plumes migrate with the flow across the Strait and through the passages between Orcas, Saturna, Mayne, and Galiano Islands into Haro Strait. In one case the tidal flow was so strong that the sediment plume could be traced as far east as the passage between Orcas and Lummi Islands (Fig. 6.7). However, the prevailing northwesterly and westerly winds averaged 30 kms/h during the 24-hour period preceding the time of image and may have added to this effect (Pacific Weather Center, Environment Canada).

Numerous cyclonic and anticylonic eddies are associated with the plumes. These eddies, which are probably the result of interactions between inertial, tidal, and coriolis forces, maintain their integrity for several hours. For instance, in Figure 6.6, a cyclonic eddy is observed in the region north of Galiano Island. Since it appears to be detached from the major plume emanating from the Fraser River, it probably represents a relict bolus that moved into the region during a previous tide. This means that at least during some seasons, boluses of low salinity water derived from the Fraser River are probably capable of maintaining their identity for periods longer than a single tidal cycle.

The sediment plume emanating from North Arm during ebb tide flows to the north and west past Point Grey (Figs. 6.6 and 6.7). Beyond Point Grey the plume bifurcates, with a portion of the plume moving to the northwest and the remaining material flowing to the northeast into Burrard Inlet.

The dispersal pattern of the Fraser River plume during flood tide has some characteristics which are very similar to the pattern for ebb tide and some which are uniquely different. As indicated in Figures 6.5 and 6.9, the sediment plumes originating from Main Arm and Middle Arm flow seaward in a southwesterly direction. However, instead of being diverted to the southeast, as is the case during ebb tide, the flood current drives the sediment plume across the Strait and to the northwest along the northern coast of Galiano Island. Some material from the plume passes into Trincomali Channel from Porlier Pass and the remaining material continues to flow to the northwest, mixing with and being diluted by the less turbid water of the northwestern Strait.

There is evidence for some small cyclonic and anticyclonic eddies in the plumes associated with the flooding tide. These eddies are interpreted as evidence for interactions between the longitudinal pressure gradient, associated with the fresh water input from the Fraser River, and the tidal and coriolis forces associated with water movement in the Strait during flood tide (Tabata, 1972). It is interesting to note that the anticyclonic eddies in the LANDSAT images are most pronounced when the tidal and coriolis forces are additive. The large anticyclonic eddy due west of Point Roberts in Figure 6.5 is an example of this situation. The plume appears to be split into two parts, presumably by tidal and coriolis forces. These processes increase the rate of lateral mixing and subsequent dilution of the plume.

The sediment plume from North Arm flows to the north around Point Grey and into Burrard Inlet during flood tide. There is no evidence from the LANDSAT images of sediment movement to the northwest during this stage of the tide.

6.3 DENSITY FRONTS

The LANDSAT images showed density fronts which separated light colored, particle-laden river water from the clearer, darker seawater. Klemas and Polis (1977) state that density fronts in estuarine waters are regions where the turbid brackish water contacts seawater. The denser seawater tends to underride the light brackish water, creating an inclined interface (Fig. 6.11). At the interface downwelling occurs in most cases, causing the inorganic and organic materials from the rivers, and any associated contaminants which have concentrated along the front such as surface films, foams, and oil slicks, to be carried down into the water column. Fronts of this type can be seen at the mouth of the Fraser River (Figs. 6.4, 6.7, 6.8 and 6.10), at Deception Pass (Fig. 6.8), in Haro and Rosario Straits (Figs. 6.4, 6.5, 6.6, 6.7 and 6.8), and in the Strait of Juan de Fuca (Figs. 6.4, 6.6 and 6.10).

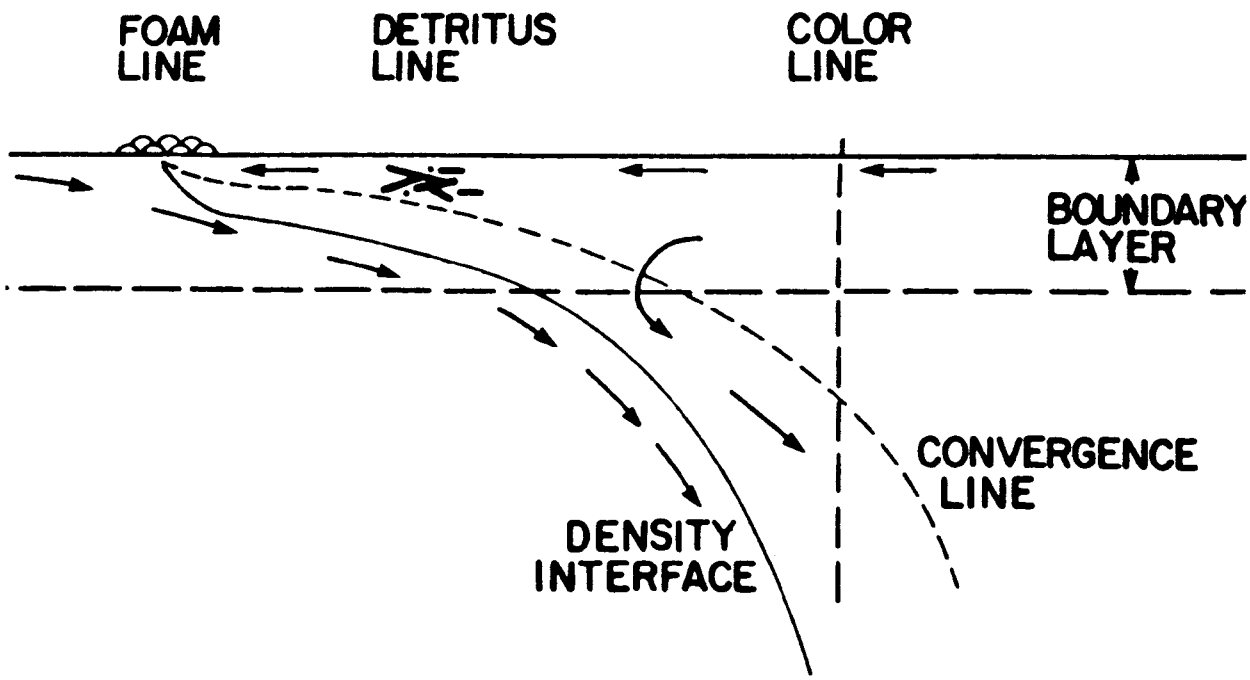

Figure 6.11 Schematic diagram of a vertical section normal to a density front (from Klemas and Polis, 1977).

In an earlier report (Cannon, Holbrook and Feely, 1978), Constance Sawyer has sketched the distribution of density fronts on charts of tidal currents from a barotropic model of the Strait of Georgia-Strait of Juan de Fuca system. The sketches are reproduced in Figures 6.13a and 6.13b. Figure 6.12 is a photograph taken from the plane on June 20, 1978, slightly northeast of Active Pass following major ebb current, showing a density front. Sawyer summarizes the distributions of the density fronts by stating that,

> Fronts are found inclined to the current at all angles, but tend to parallel the ebb current which is stronger and has stronger lateral shear. Plumes that were visible during ebb tide at Admiralty Inlet, at Deception Pass, and at the mouths of some of the smaller rivers disappeared during flood tides. Fronts parallel to strong currents appeared at the boundary of the Fraser plume (especially during flood tide), at the entrances to Haro and Rosario Straits, and in the western Strait of Juan de Fuca. The parallel fronts suggested strong cross-channel shear of the along-channel current, and the cross-channel fronts suggested a gentler sloshing back and forth of the sediment-laden water. Separation of data according to wind direction showed little dependence of frontal structure on wind.
>
> The separation of cross-channel fronts was up to 20 or 30 km. The tidal excursions estimated were 31 km for the ebb tide and 11 km for the flood, and they reasonably explained the spacing of fronts that crossed the Strait of Juan de Fuca and San Juan Island passages.

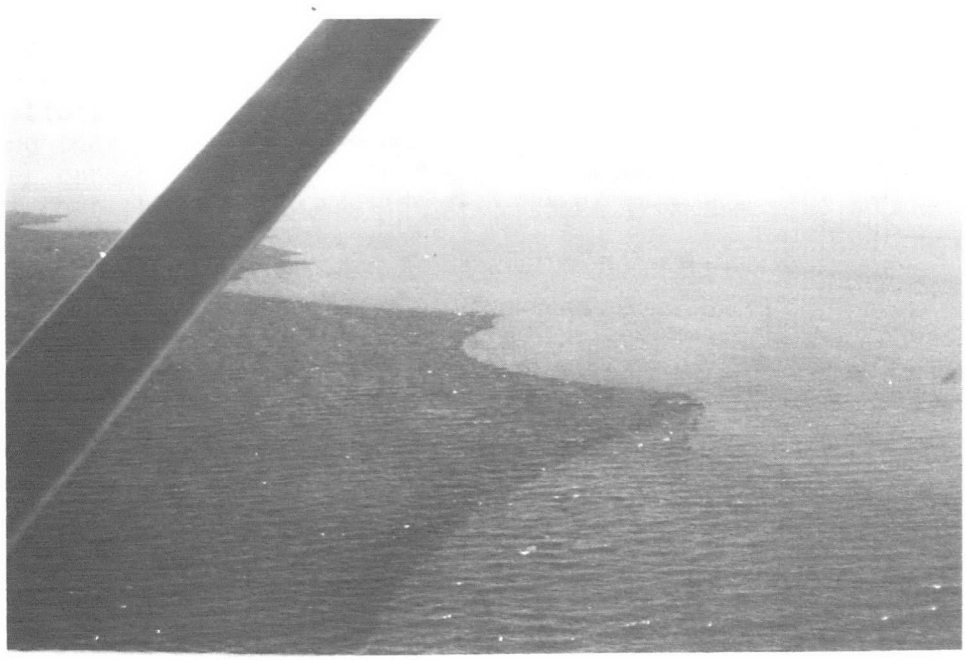

Figure 6.12. Low altitude aerial photograph showing sharp color boundary of a density front.

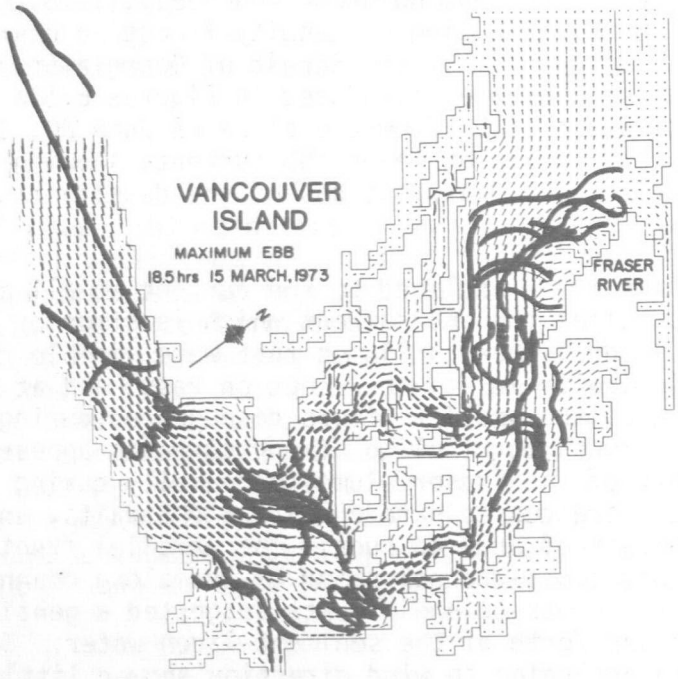

Figure 6.13a Composite sketch of fronts seen in 24 LANDSAT images during ebb tides (from Cannon et al., 1978).

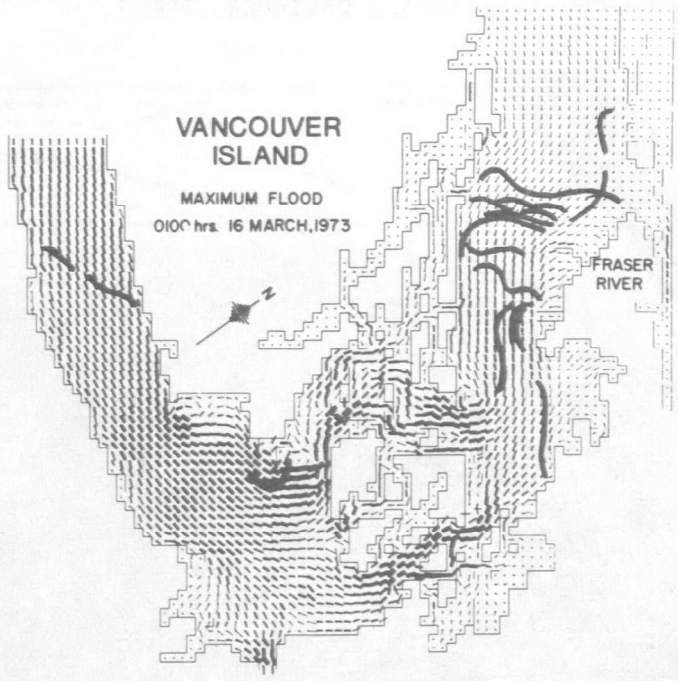

Figure 6.13b Composite sketch of fronts seen in 9 LANDSAT images during flood tides (from Cannon et al., 1978).

6.4 QUANTITATIVE SEDIMENT MAPPING

In order to develop a quantitative relationship between the image radiance from the MSS computer tapes and the sea-truth data, a stepwise multiple linear regression analysis technique was applied to the data in a manner similar to the presentation of Johnson (1975). The stepwise regression analysis program determines the one independent variable, radiance, that provides the best statistical correlation with the dependent variable, total suspended matter. The program then determines a second independent variable to be added that improves the correlation. This process is repeated until all independent variables have been included in the correlation. During each step of the process, statistical tests are performed to determine whether or not the inclusion of additional independent variables increases the correlation to a degree which is statistically significant. The data that were used for this analysis are presented in Table 6.1. The analysis was performed on the data using total suspended matter (TSM) and inorganic suspended matter (ISM) as separate dependent variables.* Tables 6.2 thru 6.5 show the results of the stepwise regression analysis of the data.

Table 6.2 shows that when TSM is the dependent variable all the MSS Bands correlate with it to some degree. The highest correlation coefficient (0.938) was associated with MSS Band 5, indicating that Band 5 may be sufficient for mapping suspended matter concentrations in northern Puget Sound. This hypothesis is supported by the standard estimate of error calculations in the stepwise regression analysis (Table 6.3), which show approximately the same standard error of estimate for a regression including only Band 5 as compared with linear combinations of the other multispectral bands. These results are substantiated by the work of Bowker et al. (1977) which demonstrated that for suspended matter concentrations below 15 mg/l in the lower Chesapeake Bay Band 5 radiance values provided the best statistical correlations. Figure 6.14a shows a plot of the relationship between Band 5 radiance in units of mW cm^{-2} $ster^{-1}$ · 100 and TSM for the three sets of sea-truth measurements. Deviations about the fitted regression line are approximately random, indicating that the linear model is adequate over the range of observed suspended matter concentrations. The good agreement for the three data sets also indicates that the linear model is consistent from one year to the next, provided atmospheric interferences are removed and the physical and chemical characteristics of the particles do not change dramatically.

Tables 6.4 and 6.5 show the results of the stepwise regression analysis using the ISM as the dependent variable. The general trend of Band 5 radiance providing the best statistical correlation is the same as the case for ISM. Furthermore, a plot of the relationship between Band 5 radiance and ISM (Fig. 6.14b) yields approximately the same slope and intercept as for TSM which means that once the data has been corrected for atmospheric interferences ISM becomes the major contributor to the observed variations of the

---

*Inorganic suspended matter concentrations were calculated by gravimetrically determining the amount of material remaining on the filters after the H_2O_2 treatment (see section 5.3).

Table 6.1 Results of sea truth measurements and remotely sensed radiances for selected locations near the mouths of the Fraser and Skagit Rivers. The station locations are shown in Figure 5.1.

Collection Date	Station	Sea Truth: Suspended Solids (mg/l)	Sea Truth: Inorganic Matter (mg/l)	Remotely Sensed Radiances ($mW \cdot cm^{-2} sr^{-1}$) · 100: Band 4	Band 5	Band 6	Band 7
June 2, 1978	2	8.594	7.600	11.8	16.7	16.2	3.3
	3	3.087	2.597	9.7	9.1	7.53	0.5
	4	5.510	4.777	9.0	8.3	6.9	0.3
	5	8.290	7.760	11.6	12.6	8.9	0.3
	6	5.576	4.710	7.3	7.4	6.8	0.2
	7	7.586	6.928	12.4	13.9	9.0	0.3
	8	6.436	5.809	11.3	12.7	7.7	0.2
	9	4.168	3.643	9.6	8.8	6.9	0.1
	10	3.285	2.025	3.2	2.7	4.4	0.1
	11	1.763	0.924	2.3	2.1	4.6	0.1
	13	3.115	2.030	4.4	4.0	5.7	0.3
July 31, 1977	1	0.490	0.250	1.3	1.7	2.4	0.0
	2	0.280	0.030	1.6	2.0	2.4	0.0
	5	0.730	0.380	4.4	4.2	3.5	0.0
	8	2.230	1.810	4.3	3.6	3.1	0.0
	9	0.720	0.380	2.8	2.6	2.9	0.0
	10	0.970	0.700	2.0	2.1	2.3	0.0
	11	0.830	0.610	2.8	2.3	2.4	0.0
	13	0.740	0.470	2.5	2.5	2.8	0.0
	14	0.740	0.460	2.2	2.3	2.7	0.0
	15	1.500	0.950	3.1	2.7	2.8	0.0
Sept 5, 1977	1	1.970	1.510	1.9	2.4	1.8	0.0
	2	0.580	0.510	1.4	1.6	1.6	0.0
	3	1.880	1.500	1.1	1.7	1.5	0.0
	5	0.770	0.630	1.6	2.0	2.2	0.0
	6	0.570	0.440	1.8	2.3	2.0	0.0
	7	0.230	1.060	1.4	2.1	2.0	0.0
	8	1.260	0.990	1.6	2.4	2.1	0.0
	9	1.880	1.300	2.1	2.9	2.3	0.0
	11	1.280	1.000	1.6	2.0	2.1	0.0
	12	1.610	1.340	1.6	1.7	2.0	0.0
	13	2.010	1.500	1.1	1.3	1.5	0.0
	15	0.310	0.230	1.4	1.9	2.2	0.0
	16	1.200	0.930	2.6	2.5	2.3	0.0
	17	2.930	2.480	5.8	6.2	4.2	0.2
	20	6.770	6.120	11.7	12.7	6.3	0.2

TABLE 6.2 Correlation coefficient matrix and linear regression equation for total suspended matter (TSM) in northern Puget Sound

	Band 4	Band 5	Band 6	Band 7	TSM
Band 4	1.000	0.977	0.924	0.630	0.938
Band 5		1.000	0.885	0.504	0.922
Band 6			1.000	0.809	0.886
Band 7				1.000	0.572
TSM					1.000

TSM = 0.0062 + 0.539 [Band 5 Radiance*]

R = 0.94

*Values corrected for atmospheric interferences.

TABLE 6.3 Results of the stepwise regression analysis of the radiance data from the MSS computer compatible tapes with the sea-truth measurements of total suspended matter

Step Number	Independent Variable Added	Regression Variable(s)	Standard Error of Estimate (mg/l)	Regression Correlation Coefficient
1	Band 5	Band 5	0.855	0.938
2	Band 4	Bands 5 and 4	0.866	0.939
3	Band 6	Bands 5, 4 and 6	0.867	0.940
4	Band 7	Bands 5, 4, 6 and 7	0.830	0.947

TABLE 6.4 Correlation coefficient matrix and linear regression equation for inorganic suspended matter (ISM) in northern Puget Sound

	Band 5	Band 4	Band 6	Band 7	ISM
Band 5	1.000	0.977	0.924	0.630	0.950
Band 4		1.000	0.885	0.504	0.927
Band 6			1.000	0.809	0.874
Band 7				1.000	0.562
ISM					1.000

$$ISM = 0.2553 + 0.5025\ [\text{Band 5 Radiance*}]$$

$$R = 0.95$$

*Values corrected for atmospheric interferences.

TABLE 6.5 Results of the stepwise regression analysis of the radiance data from the MSS computer compatible tapes with the sea-truth measurements of inorganic suspended matter

Step Number	Independent Variable Added	Regression Variable(s)	Standard Error of Estimate (mg/l)	Regression Correlation Coefficient
1	Band 5	Band 5	0.715	0.950
2	Band 4	Bands 5 and 4	0.726	0.950
3	Band 6	Bands 5, 4 and 6	0.737	0.950
4	Band 7	Bands 5, 4, 6 and 7	0.702	0.956

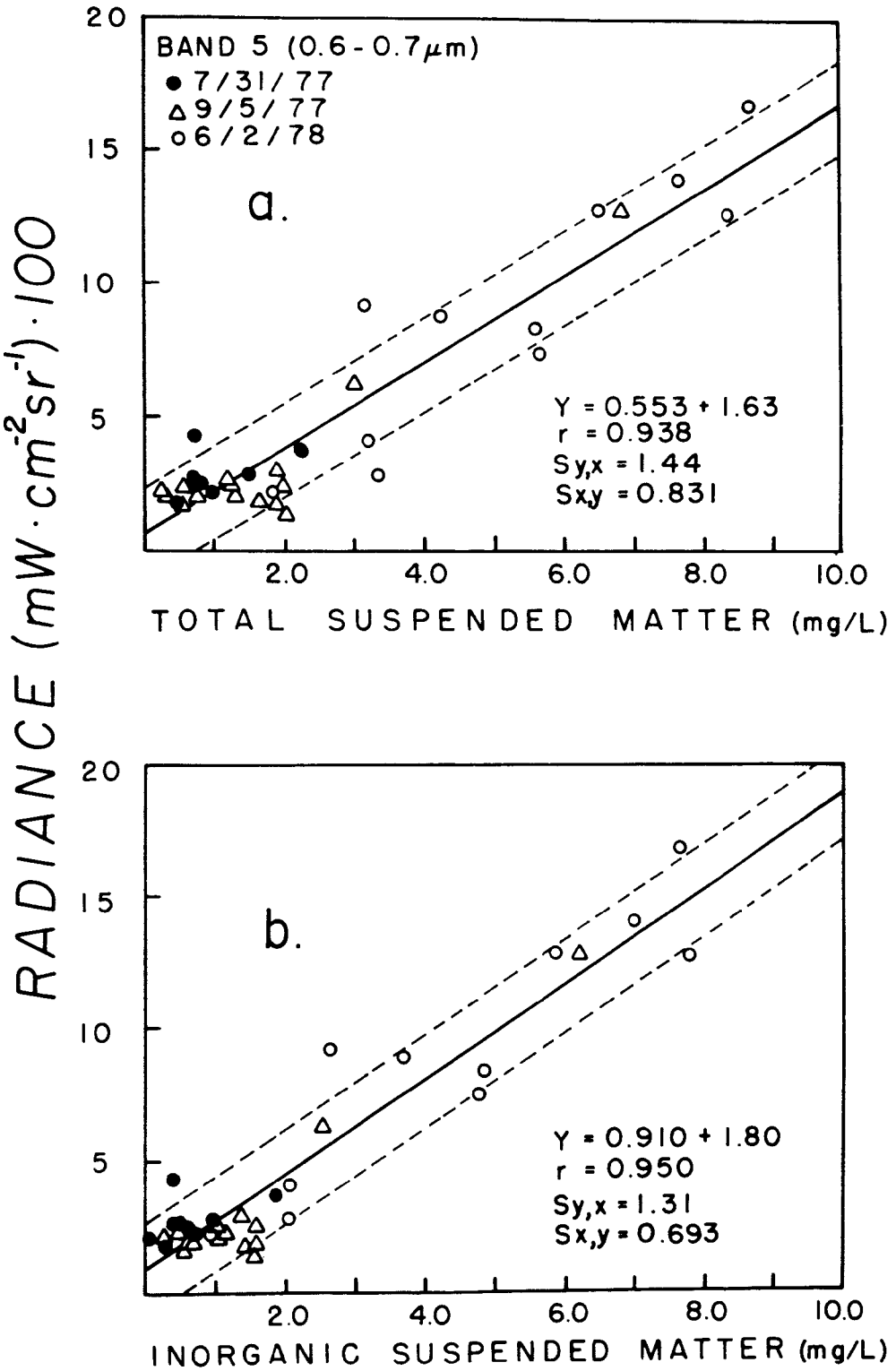

Figure 6.14 Scatter plots of the relationships among Band 5 image radiance from the LANDSAT multispectral scanner, corrected for atmospheric interferences relative to: a. total suspended matter; and b. inorganic suspended matter data obtained by gravimetric analysis of sea truth samples. The dashed lines are standard errors of estimates for the least-square fit of the data.

Band 5 radiance. This conclusion is supported by the laboratory studies of Whitlock et al. (1977) in which the reflectance of two sediments, Calvert and Ball clays, were studied as a function of wavelength. Maxima in the reflectance spectra were observed between 550 and 700 nm, with the highest peaks at about 610-680 nm (Fig. 6.15).

As indicated by the regression equation in Table 6.2, the MSS Band 5 data can be used to quantitatively map near-surface suspended matter concentrations with an estimated accuracy of about ± 20%. Figure 6.16 shows an example of a computer output based on the MSS data. The contours for TSM are fixed at 2.0 mg/l which is slightly more than twice the standard error of estimate for the fitted data and is significant at the 95% confidence level. The data are consistent with the TSM contour maps given in Baker et al. (1978) for the period using convention shipboard sampling procedures. For example, the data from July 31, 1977 (Fig. 6.16a) show the same approximate range of suspended matter concentrations (0-8 mg/l) as the field data from the August 1977 MESA cruise (Fig. 5.6a, p. 25). The computer outputs, however, provide the added advantage of supplying detailed information about the physical dimensions of the suspended matter plumes and fronts as well as allowing for estimation of concentration gradients. In Fig. 6.16b, for instance, the density front that is located in the center of the Strait of Georgia extends from a point approximately 10 km south of Point Roberts to a point approximately 15 km north of Porlier Pass, a distance of nearly 40 km. The suspended matter concentration gradient across the front is estimated to be at least 0.0024 mg/l, based on a minimum concentration difference of 2.0 mg for a distance of approximately 840 m between contour lines at some locations. This minimum estimate is limited by the resolution of the mapping procedure which means that concentration gradients in excess of this estimate could occur under normal conditions. Nevertheless, the procedure provides useful information about the physical characteristics of the density fronts which can be used to better understand the fate of suspended particles and contaminants associated with the fronts.

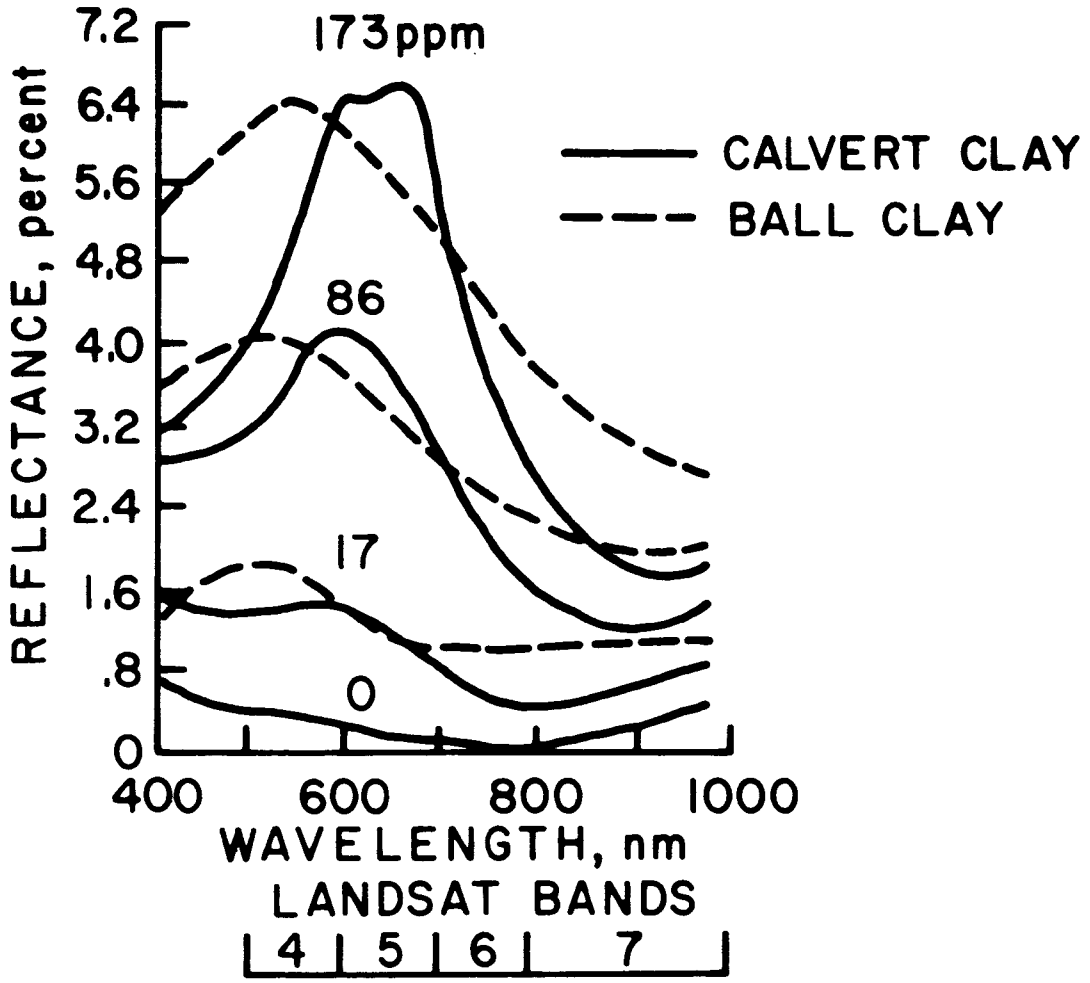

Figure 6.15 Upwelled radiance for Calvert clay and Ball clay (from Whitlock et al., 1977).

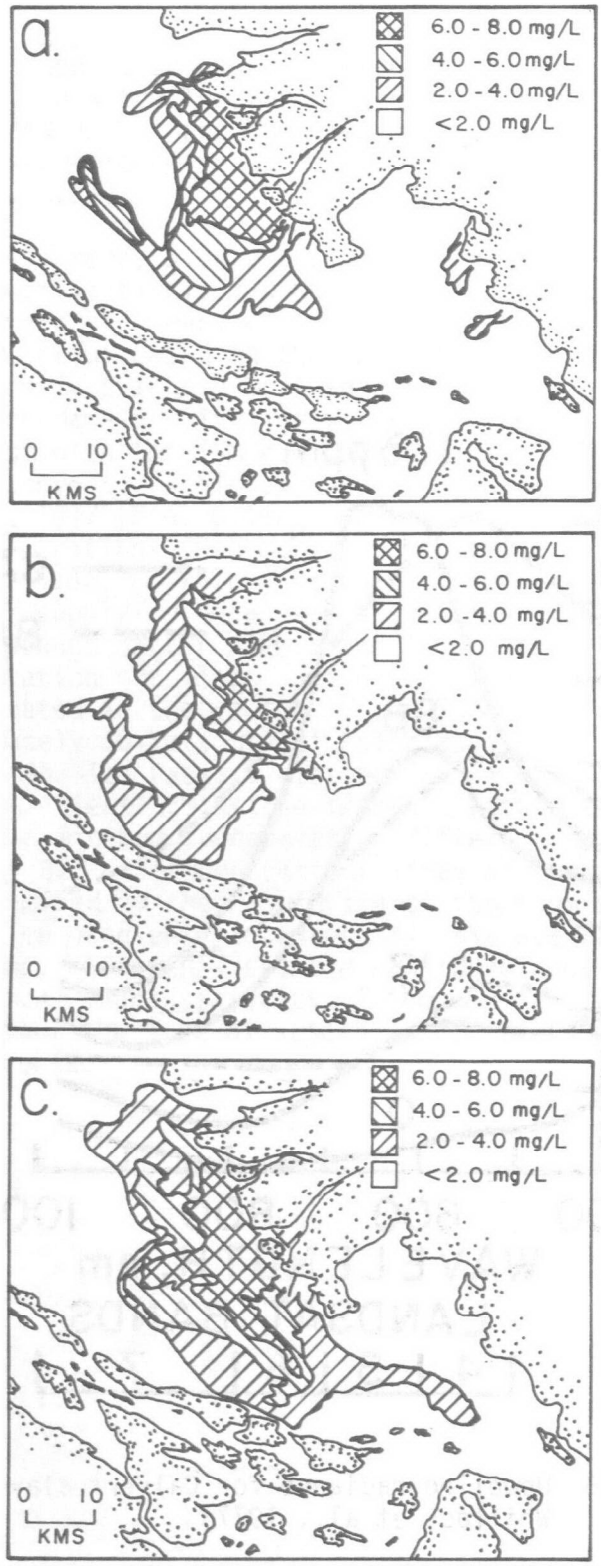

Figure 6.16. Total suspended matter contour maps as determined from computer analysis of LANDSAT images. Dates of image acqusitions are: a. July 31, 1977; b. Sept. 5, 1977; and c. June 2, 1978.

7. SUMMARY AND CONCLUSIONS

LANDSAT images, obtained during the period between 1972 and 1978, have been utilized to study the surface trajectories of sediment plumes originating from the Fraser and Skagit Rivers. These plumes are natural tracers of flow patterns of low salinity water and suspended matter that is discharged into northern Puget Sound from these rivers.

Three separate plumes can be observed emanating from the distributaries of the Fraser River. The plumes from Main Arm and Middle Arm join together to form a well-defined jet which can be traced across the Strait of Georgia and through Porlier, Active, and Boundary Passes. During ebb tide the plume is directed to the southeast from a point about midway between Steveston and Porlier Pass. The flood tide drives the plume across the Strait and to the northwest along the northern coast of Galiano Island. The presence of a well-defined jet is indicative of the significance of the longitudinal pressure and inertial forces. When water and sediment discharge is high, particularly during the spring runoff period, these forces predominate and the plumes maintain their identity for considerable distances. When discharge is low these forces are weak and tidal, coriolis, and wind forces predominate, causing rapid mixing and corresponding dilution of the plumes. The plume from North Arm moves to the northwest past Point Grey where it bifurcates, with some material flowing to the northwest during ebb tide and the remaining material moving into Burrard Inlet. The northward flow of the plume from the North Arm is probably the result of a combination of a number of forces including intertial, pressure, and coriolis.

The existence of a number of separate plumes in some of the images suggests that eddies of sediment-laden water are probably capable of maintaining their identity for periods longer than a single cycle. This implies that a dynamic balance exists between the inertial and pressure forces associated with these boluses and the coriolis and tidal forces associated with circulation patterns in the Strait. From observations of photographs taken near the mouth of Main Arm, Tabata (1972) suggests that this balance is maintained by the daily surge of fresh water from the river merging with the already present low salinity water lying along the southwestern side of the Strait. Our data support these conclusions, at least for the periods of high runoff. While the winter data are very limited, there is no evidence for multiple plumes, indicating that mixing is rapid and the lifetimes of the plumes are very short, probably less than one tidal cycle.

The plumes from the distributaries of the Skagit River are most pronounced in early summer, during the peak runoff. During this period suspended sediments from the Skagit River can be traced as far south as the middle of Saratoga Passage and as far north as Deception Pass, where Skagit River sediments flow into Rosario Strait during ebb tide. During the period of low discharge, the Skagit River plume is confined to the nearshore regions of Skagit Bay.

A stepwise multiple linear regression analysis was employed to evaluate the utility of using the digital radiance data from the MSS computer

compatible tapes for quantitatively mapping suspended matter distributions. MSS Band 5 radiance provided the best correlation with total suspended matter with estimated inaccuracy of the regression equation at about 20% (std error of estimate of 0.89 mg/l and a mean sediment weight of 4.77 mg/l in the Fraser River plume).

ACKNOWLEDGMENTS

The authors wish to express their sincere appreciation to Wally Hamilton for his technical support in developing the computer software for use in this report, and to John Truscott, Sediment Survey Section, Water Survey of Canada for his assistance in providing sediment discharge data for the Fraser River.

Gratitude is also expressed to Lake Union Air Service, Gary Massoth, Joyce Quan, Jane Hannuksela, and Ron Roberts for their help in collecting samples at the study site, and to Sharon Giese for typing the manuscript.

This work was supported by the Office of Energy, Minerals, and Industry, Office of Research and Development, U.S. Environmental Protection Agency through an interagency agreement with the Environmental Research Laboratories of NOAA.

BIBLIOGRAPHY

Baker, E. T. 1973. Distribution and Composition of Suspended Sediment in the Bottom Waters of the Washington Continental Shelf and Slope. J. Sed. Petrol. 43(3):812-821.

Baker, E. T., J. D. Cline, R. A. Feely, and J. Quan. 1978. Seasonal Distribution, Trajectory Studies, and Sorption Characteristics of Suspended Particulate Matter in the Northern Puget Sound Region, EPA 600/7-78-126, 140 p.

Bowker, D. E., and W. G. Witte. 1977. The Use of LANDSAT for Monitoring Water Parameters in the Coastal Zone. Proc. of the AIAA Joint Conference on Satellite Applications of Marine Operations, New Orleans, La.

Cannon, G. A., J. R. Holbrook, and R. A. Feely, Eds. 1978. Circulation in the Strait of Juan de Fuca: Some Recent Oceanographic Observations, NOAA Tech. Report ERL 399-PMEL 29. 94 p.

Carlson, P. R., T. J. Conomos, J. Janda, and D. H. Peterson. 1975. Principal Sources and Dispersal Patterns of Suspended Particulate Matter in Near-shore Surface Water of the Northeast Pacific Ocean, U.S.G.S. Final Report to the Goddard Flight Center.

Chang, P., S. Pond, and S. Tabata. 1976. Subsurface Currents in the Strait of Georgia, West of Sturgeon Bank. J. Fish. Res. Bd. Can. 33:2218-2241.

EPA. 1977. Review of Environmental Issues of the Transportation of Alaskan North Slope Crude Oil, EPA 600/7-77-046. Office of Energy, Minerals and Industry, Office of Research and Development, EPA, Washington, D. C. 123 p.

Feely, R. A., J. D. Cline, and G. J. Massoth. 1978. Transport Mechanisms and Hydrocarbon Adsorption Properties of Suspended Matter in Lower Cook Inlet. In: Environmental Assessment of Alaskan Continental Shelf, Environmental Research Laboratories, National Oceanic and Atmospheric Administration, Boulder, Colo.

Forrester, W. D. 1971. Distribution of Suspended Particles Following the Wreck of the Tanker "ARROW." J. Mar. Res. 29:151-170.

Gatto, L. W. 1971. Circulation and Sediment Distribution in Cook Inlet, Alaska. In: Assessment of Arctic Marine Environment Selected Types. D. W. Hood and D. C. Burrell, Eds. Occasional Pub. No. 4. Univ. of Alaska, Fairbanks, Alaska, pp. 205-228.

Herlinveaux, R. H., and J. P. Tully. 1961. Some Oceanographic Features of Juan de Fuca Strait. J. Fish. Res. Bd. Can. 18:1027-1071.

Johnson, R. W. 1975. Quantitative Sediment Mapping from Remotely Sensed Multispectral Data, Proc. Fourth Annual Remote Sensing of Earth Resources Conf., Tullahoma, Tenn.

Johnson, R. W., I. W. Duedall, R. W. Glasgow, and J. R. Proni. 1977. Quantitative Mapping of Suspended Solids in Wastewater Sludge Plumes in the New York Bight Apex. J. Water Poll. Contr. Fed. 49:2063-2073.

Klemas, V., D. Bartlett, R. Philpot, R. Rogers, and L. Reed. 1974. Coastal and Estuarine Studies with ERTS-I and Skylab. Remote Sensing of Environment. 3:153-174.

Klemas, V., and D. F. Polis. 1977. A Study of Density Fronts and Their Effects on Coastal Pollutants. Remote Sensing of Environment. 6:95-126.

Kritikos, H., L. Yorinks, and H. Smith. 1974. Suspended Solids Analysis Using ERTS-A Data. Remote Sensing of Environment. 3:95-126.

NAS. 1975. Petroleum in the Marine Environment, E. G. Wilson, Ed. National Academy of Science, Washington, D. C. 107 p.

Pacific Northwest River Basins Commission. 1970. Puget Sound Task Force. Comprehensive Study of Water and Related Land Resources, Puget Sound and Adjacent Waters, State of Washington, Appendix III, Hydrology and Natural Environment.

Parker, B. 1977. Tidal Hydrodynamics in the Strait of Juan de Fuca-Strait of Georgia. NOAA Tech. Rept. NOS-69, NOAA/DOC, Washington, D. C. 56 p.

Rouse, L. J., and T. M. Coleman. 1976. Circulation Observations in the Louisiana Bight Using LANDSAT Imagery, Remote Sensing of Environ. 5:55-66.

Schumacher, J. D., C. A. Pearson, R. A. Charnell, and N. P. Laird. 1978. Regional Response to Forcing in Southern Strait of Georgia. Estuar. Coast. Mar. Sci. 7:79-91.

Sharma, G. D., F. F. Wright, J. J. Burns, and D. C. Burbank. 1974. Sea Surface Circulation, Sediment Transport, and Marine Mammal Distribution. Alaska Continental Shelf ERTS Project 110-7, Final Report to NASA, 13 March 1974. Inst. Mar. Sci., Univ. Alaska, Fairbanks. 77 p.

Tabata, S. 1972. The Movement of Fraser River Influenced Surface Water in the Strait of Georgia as Deduced from a Series of Aerial Photographs. Dept. Environ. Water Management Service, Mar. Sci. Branch, Pac. Regional Pac. Mar. Sci., Rept. 72-6. 69 p.

Tully, J. P. 1942. Surface Non-tidal Currents in the Approaches to Juan de Fuca Strait. J. Fish. Res. Bd. Can. No. 83. 169 p.

Waldichuk, M. 1957. Physical Oceanography of the Strait of Georgia, British Columbia. J. Fish. Res. Bd. Can. 14:321-486.

Water Resources Data for Washington. 1976. U.S. Dept. Int., Geol. Surv. Water Resources Division. Tacoma, Washington.

Water Survey of Canada. Sediment Data, Canadian Rivers, Inland Waters Directorate, Ottawa, Canada, 1967-1977.

Water Survey of Canada. Water Data, Canadian Rivers, Inland Waters Directorate, Ottawa, 1967-1977.

Whitlock, C. H., J. W. Usry, W. G. Witte, and E. A. Gurganus. 1977. Laboratory Measurements of Upwelled Radiance and Reflectance Spectra of Calvert, Ball, Jordan, and Feldspar Soil Sediments. NASA TP 1039.